[26] L.V. Goodrich, R.L. Johnson, L. Milenkovic, J.A. McMahon, M.P. Scott, Conservation of the hedgehog/patched signaling pathway from flies to mice: induction of a mouse patched gene by Hedgehog, Genes Dev. 10 (1996) 301–312.
[27] Z. Burke, G. Oliver, Prox1 is an early specific marker for the developing liver and pancreas in the mammalian foregut endoderm, Mech. Dev. 118 (2002) 147–155.
[28] R. Bort, M. Signore, K. Tremblay, J.P. Martinez Barbera, K.S. Zaret, Hex homeobox gene controls the transition of the endoderm to a pseudostratified, cell emergent epithelium for liver bud development, Dev. Biol. 290 (2006) 44–56.
[29] J.K. Sicklick, Y.X. Li, A. Melhem, E. Schmelzer, M. Zdanowicz, J. Huang, M. Caballero, J.H. Fair, J.W. Ludlow, R.E. McClelland, L.M. Reid, A.M. Diehl, Hedgehog signaling maintains resident hepatic progenitors throughout life, Am. J. Physiol.: Gasterointest. Liver Physiol. 290 (2006) G859–870.
[30] N. Tanimizu, M. Nishikawa, H. Saito, T. Tsujimura, A. Miyajima, Isolation of hepatoblasts based on the expression of Dlk/Pref-1, J. Cell. Sci. 116 (2003) 1775–1786.
[31] K. Suzuki, M. Tanaka, N. Watanabe, S. Saito, H. Nonaka, A. Miyajima, p75 Neurotrophin receptor is a marker for precursors of stellate cells and portal fibroblasts in mouse fetal liver, Gastroenterology 135 (2008) 270–281 e273.
[32] H. Nonaka, M. Tanaka, K. Suzuki, A. Miyajima, Development of murine hepatic sinusoidal endothelial cells characterized by the expression of hyaluronan receptors, Dev. Dyn. 236 (2007) 2258–2267.
[33] N. Kojima, T. Kinoshita, A. Kamiya, K. Nakamura, K. Nakashima, T. Taga, A. Miyajima, Cell density-dependent regulation of hepatic development by a gp130-independent pathway, Biochem. Biophys. Res. Commun. 277 (2000) 152–158.
[34] M.J. Bitgood, L. Shen, A.P. McMahon, Sertoli cell signaling by Desert hedgehog regulates the male germline, Curr. Biol. 6 (1996) 298–304.
[35] E. Parmantier, B. Lynn, D. Lawson, M. Turmaine, S.S. Namini, L. Chakrabarti, A.P. McMahon, K.R. Jessen, R. Mirsky, Schwann cell-derived Desert hedgehog controls the development of peripheral nerve sheaths, Neuron 23 (1999) 713–724.
[36] M.A. Dyer, S.M. Farrington, D. Mohn, J.R. Munday, M.H. Baron, Indian hedgehog activates hematopoiesis and vasculogenesis and can respecify prospective neurectodermal cell fate in the mouse embryo, Development 128 (2001) 1717–1730.
[37] X. Wu, J. Walker, J. Zhang, S. Ding, P.G. Schultz, Purmorphamine induces osteogenesis by activation of the hedgehog signaling pathway, Chem. Biol. 11 (2004) 1229–1238.
[38] J.P. Incardona, W. Gaffield, R.P. Kapur, H. Roelink, The teratogenic Veratrum alkaloid cyclopamine inhibits sonic hedgehog signal transduction, Development 125 (1998) 3553–3562.
[39] A. Suzuki, Y.W. Zheng, S. Kaneko, M. Onodera, K. Fukao, H. Nakauchi, H. Taniguchi, Clonal identification and characterization of self-renewing pluripotent stem cells in the developing liver, J. Cell Biol. 156 (2002) 173–184.
[40] H.M. Holden, J.B. Thoden, F.M. Raushel, Carbamoyl phosphate synthetase: an amazing biochemical odyssey from substrate to product, Cell. Mol. Life Sci. 56 (1999) 507–522.
[41] G.R. van den Brink, Hedgehog signaling in development and homeostasis of the gastrointestinal tract, Physiol. Rev. 87 (2007) 1343–1375.
[42] S. Pathi, S. Pagan-Westphal, D.P. Baker, E.A. Garber, P. Rayhorn, D. Bumcrot, C.J. Tabin, R. Blake Pepinsky, K.P. Williams, Comparative biological responses to human Sonic, Indian, and Desert hedgehog, Mech. Dev. 106 (2001) 107–117.
[43] N. Tanimizu, H. Saito, K. Mostov, A. Miyajima, Long-term culture of hepatic progenitors derived from mouse Dlk^{+} hepatoblasts, J. Cell. Sci. 117 (2004) 6425–6434.
[44] F.P. Lemaigre, Development of the biliary tract, Mech. Dev. 120 (2003) 81–87.
[45] V.A. McLin, S.A. Rankin, A.M. Zorn, Repression of Wnt/beta-catenin signaling in the anterior endoderm is essential for liver and pancreas development, Development 134 (2007) 2207–2217.
[46] Y. Litingtung, L. Lei, H. Westphal, C. Chiang, Sonic hedgehog is essential to foregut development, Nat. Genet. 20 (1998) 58–61.
[47] J. Motoyama, J. Liu, R. Mo, Q. Ding, M. Post, C.C. Hui, Essential function of Gli2 and Gli3 in the formation of lung, trachea and oesophagus, Nat. Genet. 20 (1998) 54–57.

Development 137, 159-167 (2010) doi:10.1242/dev.041574

A novel regulatory mechanism for Fgf18 signaling involving cysteine-rich FGF receptor (Cfr) and delta-like protein (Dlk)

Yuichiro Miyaoka[1], Minoru Tanaka[2], Toru Imamura[3], Shinji Takada[4,5] and Atsushi Miyajima[1,*]

SUMMARY

Fibroblast growth factors (FGFs) transduce signals through FGF receptors (FGFRs) and have pleiotropic functions. Besides signal-transducing FGFRs, cysteine-rich FGF receptor (Cfr; Glg1) is also known to bind some FGFs, although its physiological functions remain unknown. In this study, we generated *Cfr*-deficient mice and found that some of them die perinatally, and show growth retardation, tail malformation and cleft palate. These phenotypes are strikingly similar to those of *Fgf18*-deficient mice, and we revealed interaction between Cfr and Fgf18 both genetically and physically, suggesting functional cooperation. Consistently, introduction of Cfr facilitated Fgf18-dependent proliferation of Ba/F3 cells expressing Fgfr3c. In addition, we uncovered binding between Cfr and delta-like protein (Dlk), and noticed that *Cfr*-deficient mice are also similar to *Dlk*-transgenic mice, indicating that Cfr and Dlk function in opposite ways. Interestingly, we also found that Dlk interrupts the binding between Cfr and Fgf18. Thus, the Fgf18 signaling pathway seems to be finely tuned by Cfr and Dlk for skeletal development. This study reveals a novel regulatory mechanism for Fgf18 signaling involving Cfr and Dlk.

KEY WORDS: Cysteine-rich FGF receptor (Cfr), Delta-like protein (Dlk), Fibroblast growth factor 18 (Fgf18)

INTRODUCTION

The fibroblast growth factor (FGF) family consists of 22 members in mice and humans, and has pleiotropic roles. Gene targeting studies have clearly demonstrated that some FGFs are indispensable to the development of many organs and tissues, including the limbs, lungs, liver, brain, testes, hair follicles and skeleton (Eswarakumar et al., 2005). FGFs transduce intracellular signals via FGF receptors (FGFRs) with a tyrosine kinase. As there are four genes encoding FGFRs in mice and humans, and Fgfr1, Fgfr2 and Fgfr3 each have two splice variants, the FGFR family consists of seven members. Each FGFR binds a subset of FGFs and transduces signals by forming an active receptor complex (Eswarakumar et al., 2005). Besides FGFRs, there are several FGF-binding molecules that also contribute to FGF signaling. Heparan sulfate proteoglycans (HSPGs) are necessary for the dimerization and activation of FGFRs by FGFs (Spivak-Kroizman et al., 1994; Yayon et al., 1991). Klothos are transmembrane proteins that modify the specificity of FGFRs by forming complexes with them and are indispensable for signaling by the FGFs with endocrine functions: i.e. Fgf19 (Fgf15 – Mouse Genome Informatics), Fgf21 and Fgf23 (Kurosu et al., 2007; Kurosu et al., 2006; Suzuki et al., 2008b; Urakawa et al., 2006). FGFR-like 1 (Fgfrl1), which shares sequence homology with FGFRs in its extracellular domain, but lacks an intracellular tyrosine-kinase, is also involved in FGF signaling (Wiedemann and Trueb, 2000). FGFRL1 seems to be a decoy receptor that negatively regulates FGF signaling (Trueb et al., 2003), and has indispensable roles in the development of the diaphragm (Baertschi et al., 2007). Thus, the modulation of FGF signaling by FGF-binding molecules plays important roles in normal developmental processes.

Cysteine-rich FGF receptor (Cfr; Glg1 – Mouse Genome Informatics) is another non-FGFR FGF-binding molecule, which was identified as a transmembrane molecule with affinity for Fgf1 and Fgf2 (Burrus and Olwin, 1989), and subsequently shown to bind Fgf3 and Fgf4 (Burrus et al., 1992; Kohl et al., 2000). Although Cfr binds FGFs via its large extracellular domain consisting of 16 repeats of an unique motif known as the Cfr repeat, it has no sequence homology with FGFRs and its intracellular domain consists of a short peptide of 13 amino acids without a kinase (Zhou et al., 1997). Thus, Cfr is a unique FGF-binding protein and may play a role in FGF signaling like the other FGF-binding proteins described above; however, its functions remain to be elucidated.

In this study, we identified Cfr as a delta-like protein (Dlk)-binding molecule. Dlk, also known as preadipocyte factor 1 (Pref-1), is a transmembrane protein with six epidermal growth factor (EGF) repeats in its extracellular domain. Dlk has sequence homology with Delta, a ligand for Notch, but lacks the Delta/Serrate/LAG-2 (DSL)-motif required for the activation of Notch. Dlk is abundantly expressed in various embryonic tissues (Smas and Sul, 1993) and we previously identified Dlk as a cell surface marker for hepatoblasts, embryonic hepatic progenitor cells (Tanimizu et al., 2003). *Dlk*-deficient mice show several developmental abnormalities such as perinatal death, growth retardation, skeletal abnormalities, increased amounts of adipose tissue and abnormal B cell development (Moon et al., 2002; Raghunandan et al., 2008), indicating that Dlk plays a fundamental role in development. Having identified Cfr as a Dlk-binding protein, we were interested in the functions of Cfr and the relation between Cfr and Dlk. To reveal the functions of Cfr, we generated *Cfr*-deficient mice and found that some of them die shortly after birth and show growth retardation, tail distortion and cleft palate. Among all the *Fgf*-deficient mice published, *Fgf18*-deficient mice were most similar to *Cfr*-deficient mice in terms of these

[1]Laboratory of Cell Growth and Differentiation, Institute of Molecular and Cellular Biosciences and [2]Promotion of Independence for Young Investigators, The University of Tokyo, Yayoi, Bunkyo-ku, Tokyo 113-0032, Japan. [3]Signaling Molecules Research Laboratory, National Institute of Advanced Industrial Science and Technology (AIST), Tsukuba, Ibaraki 305-8566, Japan. [4]Okazaki Institute for Integrative Biosciences, National Institutes of Natural Sciences, and [5]Department of Basic Biology, Graduate University for Advanced Studies (SOKENDAI), Okazaki, Aichi 444-8787, Japan.

*Author for correspondence (miyajima@iam.u-tokyo.ac.jp)

Accepted 21 October 2009

phenotypes (Liu et al., 2002; Ohbayashi et al., 2002). Fgf18 activates intracellular signaling mainly via Fgfr3c (Zhang et al., 2006), and it is well established that Fgf18-Fgfr3c signaling plays a central role in skeletal development (Haque et al., 2007). Fgf18 inhibits the proliferation of chondrocytes (Liu et al., 2002; Ohbayashi et al., 2002), and several Fgfr3 mutations in humans are known to be a cause of dwarfism (Horton et al., 2007). In this paper, we show genetic and physical interaction between Cfr and Fgf18, and a positive regulatory role of Cfr in Fgf18 signaling. Moreover, we also noticed that the phenotypes of *Cfr*-deficient mice are similar to those of *Dlk*-transgenic mice (Lee et al., 2003) and found that Dlk inhibits the physical interaction between Cfr and Fgf18. Taken together, these results imply that Dlk interferes with the positive regulatory role of Cfr in Fgf18 signaling by abrogating the binding between Cfr and Fgf18. Thus, our study reveals a novel regulatory mechanism for Fgf18 signaling involving Cfr and Dlk.

MATERIALS AND METHODS

Mice

Cfr-deficient mice were generated by using a gene-trapped 129Ola embryonic stem (ES) cell line (see Results). The cell line used for this research project, BayGenomics clone KST005 (catalog number 000716-UCD), was obtained from the Mutant Mouse Regional Resource Center (MMRRC), a NCRR-NIH funded strain repository, and was donated to the MMRRC by the NIH and NHLBI supported BayGenomics consortium. The mouse model will be made available (BRC No. RBRC03897) from the RIKEN BioResource Center (RIKEN BRC), which is participating in the National Bio-Resource Project of the MEXT, Japan, please contact them at animal@brc.riken.jp for inquiries, or search the catalog at http://www.brc.riken.go.jp/lab/animal/en/. The details of *Fgf18* targeting were described previously (Ohbayashi et al., 2002). The *Cfr*-mutant and *Fgf18*-mutant mice used in this study had been back crossed with C57BL/6 wild-type mice at least eight and ten times, respectively. All experimental procedures in this study were approved by the institutional animal care and use committee of the University of Tokyo.

Antibodies

The antibodies used were as follows: anti-Actin (sc-1616) purchased from Santa Cruz Biotechnology, rat monoclonal antibody against Dlk raised in our laboratory (Suzuki et al., 2008a); anti-Cfr rabbit serum raised against the N-terminal domain of Cfr without a signal sequence (28-256 amino acid residues), which was expressed in *Escherichia coli*, and anti-Fgf18 rabbit serum raised against full-length Fgf18 without a signal sequence, which was fused to a GST tag and expressed in *E. coli*.

Expression screening for Dlk-binding proteins

The extracellular domain of Dlk (1-303 amino acid residues) fused to the human IgG Fc region (Dlk-Fc) was expressed in COS7 cells and purified from the culture supernatant with a Hi Trap column (GE Healthcare), and then biotinylated with a biotinylation module (GE Healthcare) for flow cytometric analysis. First, we constructed a cDNA library of HPPL with the FastTrack 2.0 mRNA Isolation Kit (Invitrogen) and SuperScript Choice System (Invitrogen) in the pMXs retroviral vector. The plasmid was then converted to retrovirus using PLAT-E cells. Ba/F3 cells were infected with the virus library and Ba/F3 cells that bound Dlk-Fc were enriched by IMag (Becton-Dickinson) cell sorting using biotinylated Dlk-Fc protein. Genomic PCR of the sorted cells revealed that some of them had the full-length *Cfr* sequence in their genomes (see Results).

Retroviral gene transfer and proliferation assay of Ba/F3 cells

We utilized a Ba/F3 cell line, which expresses a fusion protein of the extracellular domain of Fgfr3c and the intracellular domain of Fgfr1 described previously (Ornitz et al., 1996). For simplicity, we refer to this fusion protein as Fgfr3c in this report.

We constructed a pMXs-IRES-GFP vector encoding the full-length Cfr and produced retroviruses from the vector using PLAT-E cells as described previously (Miyaoka et al., 2006). Ba/F3 cells were infected with the viruses and cells expressing GFP were sorted by FACSVantage (Becton Dickinson).

For proliferation assay, Ba/F3 cells were deprived of cytokines for at least 6 hours, and then 2×10^3 Ba/F3 cells were cultured in 100 μl RPMI-1640 (SIGMA) containing 10% fetal bovine serum (EQUITECH-BIO), 2 mM L-glutamine, 50 μg/ml gentamicin (Wako), and the indicated reagents per 96 well for 2 or 3 days. We assessed the extent of proliferation by adding 10 μl WST-1 reagent (Roche) per 96 well, incubating at 37°C for 2 hours, and monitoring absorbance at 450 nm subtracted by basal absorbance at 650 nm. We set eight wells per one condition in all the experiments in this report.

Quantitative PCR analysis

For cDNA synthesis, total RNA was isolated with TRIzol Reagent (Invitrogen), and then reverse transcribed with a High Capacity cDNA Reverse Transcription Kit (Applied Biosystems). For analysis, SYBR Premix Ex Taq (Takara) and Light Cycler (Roche) were used.

Histochemistry

For immunohistochemistry, embryos were dissected and fixed with methanol/DMSO (4:1) at 4°C overnight, and then incubated in methanol/DMSO/H_2O_2 (4:1:1) at room temperature for 8 hours. Embryos were rehydrated and incubated with primary antibodies at 4°C overnight. They were then incubated with anti-rat IgG-HRP at 4°C overnight. Signal was visualized with 0.06% DAB/0.06% $NiCl_2$ in PBS with 0.2% BSA, 0.5% Triton X-100 and 0.03% H_2O_2.

For immunofluorescent staining, embryos were dissected and fixed with Zamboni's fixative at 4°C overnight, and then gradually substituted to 20% sucrose in PBS. The samples were sectioned and incubated with 5% skimmed milk in PBS for 2 hours at room temperature. They were then incubated with first antibodies at 4°C overnight, and with second antibody conjugated with Alexa Fluor 488 or 555 (Invitrogen) for 2 hours at room temperature. The sections were embedded with Gel/Mount (Cosmo Bio) containing Hoechst 33342.

For examining β-gal activity, embryos were dissected and fixed with 4% paraformaldehyde in PBS at room temperature for 10 minutes. After being washed with PBS, they were incubated in 1 mg/ml X-Gal, 5 mM ferricyanide, 5 mM ferrocyanide, 2 mM $MgCl_2$, 0.02% Nonidet-P 40 and 40 mM HEPES in PBS at 37°C for appropriate periods.

Western blot analysis and northern blot analysis

The detailed methods for western blot analysis and northern blot analysis were described previously (Miyaoka et al., 2006).

Alcian Blue/Alizarin Red staining of cartilage and bone

Mice were dissected, eviscerated, and fixed with 95% ethanol overnight. They were then incubated in acetone overnight. After a brief rinse with water, the samples were incubated in 20% acetate, 75% ethanol and 0.15 mg/ml Alcian Blue 8GX overnight. Then, the samples were washed with 70% ethanol for 8 hours, and cleared with 1% KOH overnight. For counterstaining, 0.05 mg/ml Alizarin Red in 1% KOH was used, and the samples were cleared in 1% KOH in 20% glycerol. All steps were done at room temperature.

Immunoprecipitation

The extracellular domain of Cfr (1-869 amino acid residues) fused tandemly to a His tag and a FLAG tag at its C-terminus (Cfr-EC) was expressed in COS7 cells and purified by using His Trap column (GE Healthcare). Protein G Sepharose (GE Healthcare) was used for precipitation of Fc-fused proteins. Cfr-EC was immunoprecipitated with anti-Cfr serum and protein G Sepharose, or anti-FLAG M2 agarose (SIGMA). These beads were incubated with culture supernatants or the lysis buffer (Miyaoka et al., 2006) containing their target proteins at 4°C for 4 hours, and then washed with the lysis buffer four times.

RESULTS

Identification of Cfr as a Dlk-binding molecule

First, we attempted to identify molecules that bind to Dlk by using an expression screening method. To find cells expressing Dlk-binding proteins on their surface, the extracelluar domain of Dlk

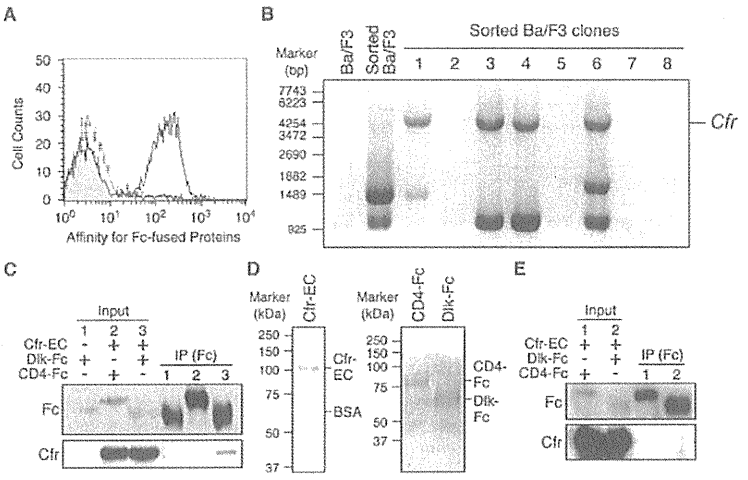

Fig. 1. Identification of Cfr as a Dlk-binding molecule. (**A**) Flow cytometric analysis of the binding of Dlk-Fc protein to HPPL. The specificity of the binding was confirmed with control CD4-Fc protein. Grey, no protein added; dotted line, CD4-Fc; unbroken line, Dlk-Fc. (**B**) DNA fragments inserted by retroviruses in Ba/F3 clones isolated by the cell sorting. Virus-sequence-specific primers amplified the inserted DNA fragments by PCR. Ba/F3, untreated Ba/F3 cells; sorted Ba/F3 cells, the sorted bulk Ba/F3 cells before cloning. (**C**) Immunoprecipitation confirming the binding between Dlk and Cfr. Plasmid constructs shown were introduced into COS7 cells, and Dlk-Fc or CD4-Fc was immunoprecipitated from the culture supernatants. Western blot analysis revealed that the extracellular domain of Cfr (Cfr-EC) was specifically co-immunoprecipitated with Dlk-Fc. (**D**) Coomassie Brilliant Blue staining of Cfr-EC, CD4-Fc and Dlk-Fc purified from COS7 culture supernatants. A weak signal of residual BSA was observed together with that of Cfr-EC. (**E**) Western blot analysis of the immunoprecipitates confirming the binding between the purified Dlk-Fc and Cfr-EC.

was fused to the Fc domain of human IgG (Dlk-Fc) and flow cytometry was used to find cells that bound Dlk-Fc. We found that Dlk-Fc strongly bound to HPPL, a hepatocyte progenitor cell line (Tanimizu et al., 2004) (Fig. 1A). To clone a cDNA encoding the Dlk-binding protein, a retroviral cDNA expression library was constructed from HPPL and introduced into Ba/F3 cells. Magnetic cell sorting was used to enrich Ba/F3 cells that bound Dlk-Fc. After three rounds of enrichment, we obtained several Ba/F3 clones that bound Dlk-Fc. Oligonucleotide primers specific for the retrovirus sequence were used to amplify the sequences introduced into the Ba/F3 genomes by the retrovirus. Sequencing of the amplified DNA fragments revealed that four of the eight clones contained in their genomes a full-length *Cfr* cDNA sequence (Fig. 1B). Other amplified DNA fragments seemed to be non-specific, because they were all truncated, not full-length fragments, and some of them were inserted in the reverse orientation to the retrovirus promoter (data not shown). As clones 1, 3 and 4, and 6 in Fig. 1B had different non-specific fragments inserted in the genomes, these clones were independently generated and acquired the affinity for Dlk-Fc by the *Cfr* insertion. We confirmed binding between Cfr and Dlk by immunoprecipitation. The extracellular domain of Cfr (Cfr-EC) was expressed in COS7 cells together with either Dlk-Fc or the extracellular domain of CD4 fused to the Fc domain of human IgG (CD4-Fc), and the Fc-fusion proteins were immunoprecipitated from the culture supernatants. As shown in Fig. 1C, Cfr-EC was co-precipitated with Dlk-Fc but not CD4-Fc. Then, we purified Cfr-EC, Dlk-Fc and CD4-Fc, and found that the purified Cfr-EC was also co-precipitated with the purified Dlk-Fc (Fig. 1D,E). These results indicate that Cfr directly interacts with Dlk. However, as the signal of the co-precipitated purified Cfr was relatively weak compared with that from the crude culture supernatants (Fig. 1C,E), it might be possible that the interaction is enhanced by other factors.

Generation of *Cfr*-deficient mice

As there has been no report on the physiological role of Cfr, we generated *Cfr*-deficient mice by utilizing a gene-trapped ES cell line. Because this ES cell line has a *β-geo* cassette with a splice acceptor inserted in the first intron of the *Cfr* locus, normal splicing between the first and second exons was interrupted, resulting in the production of a protein in which the peptide from the first exon is fused with β-geo (Fig. 2A). The ES cells were introduced into C57BL/6 blastocysts to generate chimeric mice, and a mouse with ES-cell-derived cells in its germline was obtained. First, we confirmed the site of the *β-geo* cassette in the first intron of the *Cfr* locus by inverse PCR (data not shown), and located it, in the correct orientation, about 10 kbp 3′ downstream from the end of the first exon (Fig. 2A). The insertion was further confirmed to be correct by PCR with primers indicated in Fig. 2A (Fig. 2B). To confirm the abrogation of Cfr protein expression, lysates from embryonic day 11.5 (E11.5) whole embryos of each genotype were subjected to a western blot analysis with antiserum raised against the N-terminal domain of Cfr. An embryo homozygous for the gene-trapped allele showed a protein larger than the wild-type Cfr, the molecular weight of which corresponds to that of a fusion protein comprising the peptide from the first exon of *Cfr* and β-geo. Both the intact Cfr and the fusion protein were detected in a heterozygous embryo (Fig. 2B). Because no intact Cfr protein was detected in the embryo homozygous for the gene-trapped allele, and the first exon of *Cfr* contains only its signal peptide with a few additional amino acid residues (117 amino acid residues), it is highly likely that the gene-trap results in a null mutation. Therefore, we refer to the gene-trapped allele as '-' hereafter. Mating between $Cfr^{+/-}$ mice resulted in the generation of embryos with the normal Mendelian segregation pattern until E18.5; however, about 90% of $Cfr^{-/-}$ mice died within 2 days after birth and there were only a few $Cfr^{-/-}$ mice alive at 3

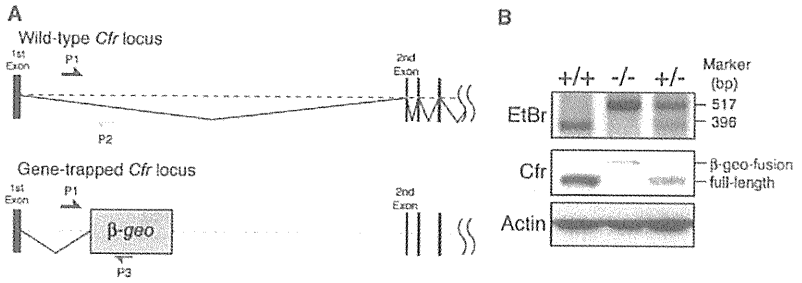

Fig. 2. Generation of Cfr-deficient mice. (**A**) Schematic representation of the wild-type and gene-trapped *Cfr* locus. The genomic region around the first intron is shown. In the trapped allele, a *β-geo* cassette is inserted in the first intron. To confirm the correct insertion, three oligonucleotide primers, P1-P3, were designed. (**B**) Confirmation of the gene-trapping. PCR with P1-P3 revealed that DNA fragments of the sizes expected from the genotypes were correctly amplified. The sizes of DNA fragments amplified with P1 and P2, and P1 and P3, should be 353 and 500 bp, respectively. The positions of DNA size markers are shown on the right. Western blot analysis of whole embryo lysate from each genotype with anti-Cfr serum revealed that the wild-type Cfr and the β-geo fusion proteins were expressed in the expected pattern from the wild-type allele and the trapped allele, respectively. No wild-type Cfr was detected in –/– embryos, indicating that this trapping resulted in a null mutation. The amount of protein loaded on the gel was confirmed by anti-actin blotting.

weeks of age (Table 1). Adult $Cfr^{-/-}$ mice had no obvious abnormality in their appearance, but their size and weight were significantly smaller than those of wild-type mice (data not shown). As a preliminary histological analysis of two $Cfr^{-/-}$ adult male survivors showed no obvious pathological abnormality in the brain, heart, lung, liver, spleen, kidney, stomach, guts, thymus, skin, skeletal muscle, eye or testis (data not shown), the cause of lethality is currently unknown. Because we identified Cfr as a Dlk-binding molecule, we considered the possibility that the lack of Cfr might affect the expression of Dlk. However, neither the mRNA nor protein level of Dlk was altered in *Cfr*-deficient mice (see Fig. S1A-D in the supplementary material). Because the inserted *β-geo* cassette expresses β-gal activity via the promoter of the inserted gene, the β-gal activity in $Cfr^{+/-}$ embryos represents the *Cfr* promoter activity. At E7.5, *Cfr* was expressed only in the epiblast, and thereafter ubiquitously at all stages examined, E8.5-14.5 (see Fig. S2A in the supplementary material and data not shown). Northern blot analysis using total RNA from various adult tissues revealed that *Cfr* was expressed in all the tissues examined, although levels were variable (see Fig. S2B in the supplementary material). Thus, Cfr is expressed broadly in the body from early embryonic stages to adulthood.

Growth retardation, skeletal abnormality and cleft palate in *Cfr*-deficient mice

At E18.5, $Cfr^{-/-}$ embryos were smaller in size and weighed less than $Cfr^{+/+}$ and $Cfr^{+/-}$ littermates (Fig. 3A,B). We also noticed that tails of all $Cfr^{-/-}$ E18.5 embryos and neonates were distorted, suggesting an abnormal skeletal development. In fact, Alcian Blue/Alizarin Red staining of bones and cartilages revealed that tail skeletons of $Cfr^{-/-}$ neonates were distorted, whereas the other skeletons were almost normal (Fig. 3C). The distortion seemed to be caused by an irregular arrangement of the tail cartilages (Fig. 3D). In addition, about 19% (7/37) of $Cfr^{-/-}$ neonates had a bloated abdomen filled with air (Fig. 3E). As cleft palate in mice often results in an accumulation of air in the stomach and a bloated abdomen, we investigated the palates of $Cfr^{-/-}$ neonates, and found that about 30% (11/37) of the mice exhibited cleft palate (Fig. 3F). All of the $Cfr^{-/-}$ mice with a bloated abdomen had a cleft palate. We investigated craniofacial skeletal elements and found incomplete fusion of maxillary shelves in $Cfr^{-/-}$ neonates with cleft palate (Fig. 3G). The other skeletal elements were apparently normal in $Cfr^{-/-}$ mice (Fig. 3C,G and data not shown). $Cfr^{+/-}$ mice showed no obvious abnormality. These results indicate that Cfr is essential for normal development.

Expression profile of Cfr and Dlk in developing skeletons

Although Cfr is ubiquitously expressed in embryos, as shown in Fig. S2 in the supplementary material, the skeletal abnormality of $Cfr^{-/-}$ mice prompted us to investigate more detailed expression patterns of Cfr in embryonic skeletons. We examined expression patterns of Cfr as well as Dlk in limbs, vertebrae and maxillae of E14.5 wild-type embryos by immunofluorescent staining and found that Cfr and Dlk were specifically expressed in prehypertrophic chondrocytes, and reserve and proliferating chondrocytes, respectively, in humeri (Fig. 4). The same expression patterns were observed in other limb skeletons (data not shown). Cfr and Dlk were also expressed in vertebrae and maxillae, although the specificity of cell-types or stages was unclear (see Fig. S3A,B in the supplementary material). Thus, Cfr and Dlk are expressed in developing skeletons, contributing to skeletal development.

Table 1. Genotypes of offspring from matings of $Cfr^{+/-}$ mice

	E9.5	E18.5	P0	P1	P2	3 week
+/+	26 (25.2)	32 (25.8)	40 (30.8)	32 (30.2)	76 (36.7)	63 (32.0)
+/–	51 (49.5)	57 (46.0)	70 (53.8)	69 (65.1)	124 (59.9)	129 (65.5)
–/–	26 (25.2)	35 (28.2)	20 (15.4)	5 (4.7)	7 (3.4)	5 (2.5)
Total	103	124	130	106	207	197

Male and female $Cfr^{+/-}$ mice were mated and genotypes of the offspring were analyzed at the indicated time points. The numbers in parentheses indicate the percentage of a genotype. The Mendelian segregation pattern was observed until E18.5, but the number of $Cfr^{-/-}$ mice was reduced after birth. By day 2 after birth, about 90% of $Cfr^{-/-}$ mice had died.

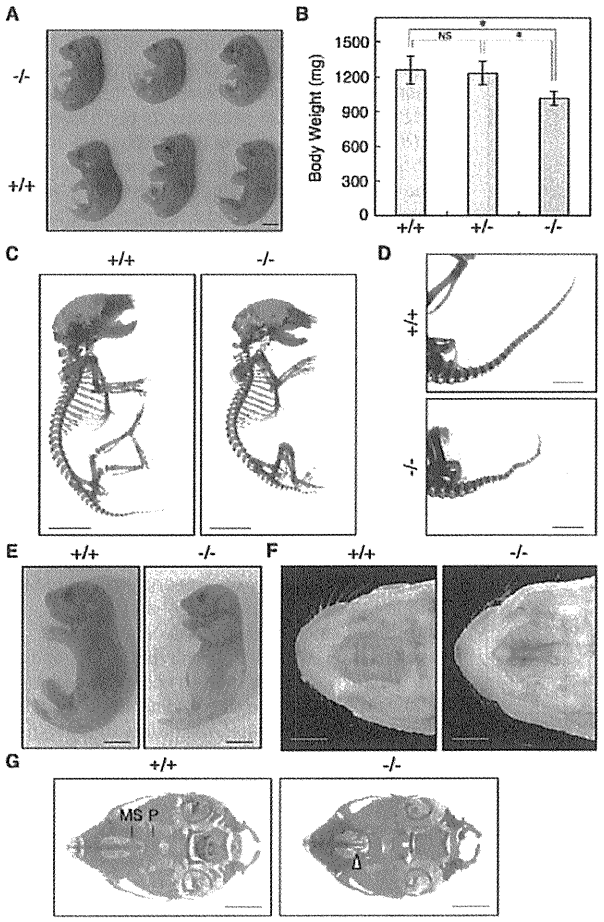

Fig. 3. Phenotypes of *Cfr*-deficient mice. (**A**) E18.5 $Cfr^{+/+}$ (lower three) and $Cfr^{-/-}$ (upper three) littermates. Note that the $Cfr^{-/-}$ embryos are smaller. (**B**) Body weight of E18.5 embryos with s.d. (+/+, n=25; +/–, n=46; –/–, n=30). P-value was calculated with Student's t-test: *, P<0.001; NS, P>0.5. (**C**) Alcian Blue/Alizarin Red staining of bone and cartilage of neonates. $Cfr^{-/-}$ neonates showed a basically normal skeleton except for their distorted tails. (**D**) Distorted tails of $Cfr^{-/-}$ neonates. All $Cfr^{-/-}$ neonates had a distorted tail. (**E**) Bloated abdomen of $Cfr^{-/-}$ neonates. About 19% (7/37) of $Cfr^{-/-}$ neonates had a bloated abdomen filled with air. (**F**) Cleft palate of $Cfr^{-/-}$ neonates. About 30% (11/37) of $Cfr^{-/-}$ neonates had a cleft palate. (**G**) Incomplete fusion of maxillary shelves in about 25% (3/13) of $Cfr^{-/-}$ neonates. Craniofacial skeletons were stained with Alcian Blue/Alizarin Red and viewed from beneath. For clarity, the lower jaws were removed. The arrowhead indicates the incomplete fusion of maxillary shelves. Scale bars: 2 mm in D,F,G; 5 mm in A,C,E. MS, maxillary shelves; P, palatine.

Genetic interaction between *Cfr* and *Fgf18*

Because Cfr is an FGF-binding molecule, we considered that the observed phenotypes of *Cfr*-deficient mice were caused by deregulation of some of the FGF signaling pathways. To address this possibility, we compared *Cfr*-deficient mice with all the *Fgf*-deficient mice reported previously, and noticed that the phenotypes of $Cfr^{-/-}$ mice, such as perinatal death, growth retardation, tail distortion and cleft palate, are markedly similar to those of *Fgf18*-deficient mice. Therefore, we searched for a

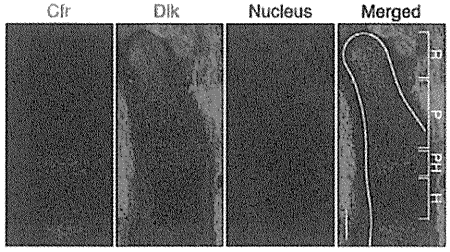

Fig. 4. Expression profiles of Cfr and Dlk in humeri. Immunofluorescent staining of Cfr (green) and Dlk (red) in E14.5 wild-type humeral longitudinal sections. In the merged photograph, the green and red signals are merged with signals of nuclei stained with Hoechst 33342 (blue), and humeri are outlined by a white line. Regions for reserve (R), proliferating (P), prehypertrophic (PH) and hypertrophic (H) chondrocytes are indicated. Note that Cfr is expressed specifically in prehypertrophic chondrocytes, while Dlk in reserve and proliferating chondrocytes. Scale bar: 80 μm.

functional link between Cfr and Fgf18. First, we investigated whether there is any genetic interaction between *Cfr* and *Fgf18* by mating $Cfr^{+/-}$ mice with $Fgf18^{+/-}$ mice. Among the offspring, wild-type, $Cfr^{+/-}$ and $Fgf18^{+/-}$ mice had no obvious phenotype. $Cfr^{+/-}$;$Fgf18^{+/-}$ double heterozygous (D-HT) mice were viable and fertile (data not shown). They were comparable in body weight to other genotypes and had a normal tail morphology at birth (see Fig. S4A,B in the supplementary material). However, D-HT mice were significantly smaller than wild-type mice at 3 months after birth, whereas neither $Cfr^{+/-}$ nor $Fgf18^{+/-}$ mice showed such a phenotype (Fig. 5A). The phenotype was more evident in D-HT male mice, as they were already smaller than wild-type male mice at 1 month after birth (Fig. 5A). Moreover, the tails of D-HT mice were distorted by 7 days after birth like those of *Cfr*-deficient mice and *Fgf18*-deficient mice, but neither $Cfr^{+/-}$ nor $Fgf18^{+/-}$ mice showed tail distortion (Fig. 5B,C). The tail distortion in D-HT mice was visible from postnatal day 3 and retained even in adulthood. About 83% (19/23) of adult D-HT mice showed the malformation. These phenotypes clearly indicate genetic interaction between *Cfr* and *Fgf18*, suggesting functional cooperation.

We further analyzed the genetic interaction between *Cfr* and *Fgf18* by crossing D-HT mice. As was the case for the offspring from mating of $Cfr^{+/-}$ mice (Table 1), some $Cfr^{-/-}$ neonates from mating of D-HT mice died after birth. Mortality among $Cfr^{-/-}$;$Fgf18^{+/-}$ mice was similar to that among $Cfr^{-/-}$ mice, indicating that the lack of one *Fgf18* allele did not affect the viability of $Cfr^{-/-}$ mice (data not shown). Likewise, skeletons of $Cfr^{-/-}$ and $Cfr^{-/-}$;$Fgf18^{+/-}$ neonates showed no significant difference (Fig. 5D). Consistent with the finding that the complete loss of *Fgf18* resulted in perinatal death and skeletal abnormalities (Liu et al., 2002; Ohbayashi et al., 2002), $Cfr^{+/-}$;$Fgf18^{-/-}$, $Cfr^{-/-}$;$Fgf18^{-/-}$ as well as $Fgf18^{-/-}$ mice died at birth. $Fgf18^{-/-}$ neonates showed slightly distorted ribs and the additional loss of one *Cfr* allele ($Cfr^{+/-}$;$Fgf18^{-/-}$) enhanced the distortion of the ribs and caused curvature of the spine. In $Cfr^{-/-}$;$Fgf18^{-/-}$ double knockout neonates, the distortion of the ribs and curvature of the spine were much more severe than in $Cfr^{+/-}$;$Fgf18^{-/-}$ mice, although the number of ribs was normal and there was no fusion of the ribs (Fig. 5D). These results clearly indicate that Cfr and Fgf18 play indispensable and overlapping roles in skeletal development.

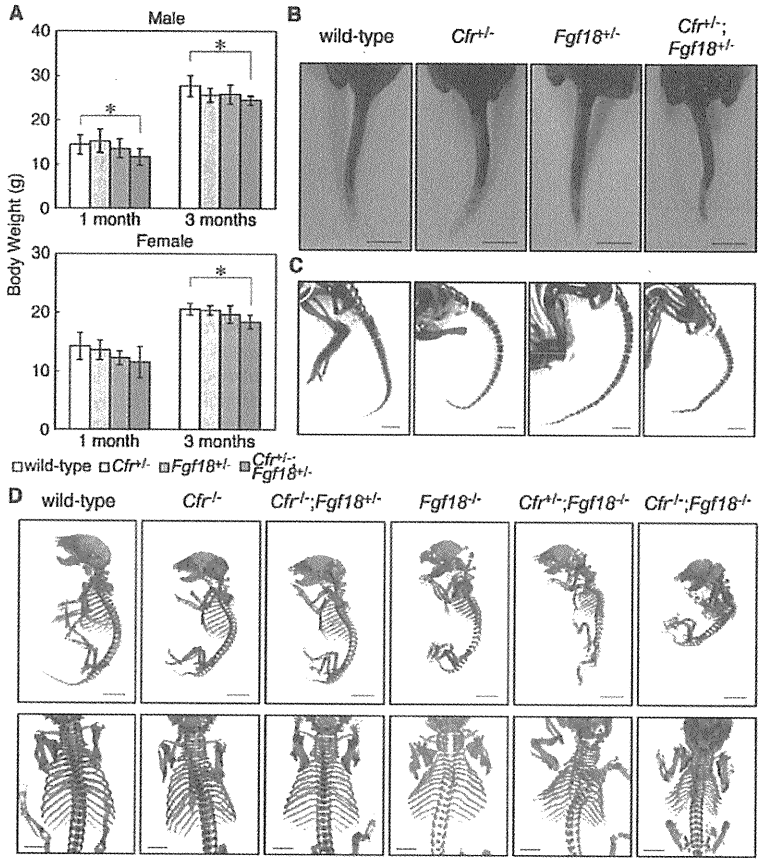

Fig. 5. Genetic interaction between *Cfr* and *Fgf18*. (**A**) Body weight of wild-type, *Cfr*$^{+/-}$, *Fgf18*$^{+/-}$ and *Cfr*$^{+/-}$;*Fgf18*$^{+/-}$ (double heterozygous, D-HT) 1 and 3 month(s) old mice from the mating of *Cfr*$^{+/-}$ and *Fgf18*$^{+/-}$ mice with s.d. (wild-type, *n*=6; *Cfr*$^{+/-}$, *n*=7; *Fgf18*$^{+/-}$, *n*=8; D-HT, *n*=6 for male) (wild type, *n*=5; *Cfr*$^{+/-}$, *n*=9; *Fgf18*$^{+/-}$, *n*=6; D-HT, *n*=9 for female). *P*-value was calculated with Student's *t*-test, *, $P<0.05$. Other *P*-values between wild-type mice and mutant mice are more than 0.07. (**B**) Tail morphology of wild-type, *Cfr*$^{+/-}$, *Fgf18*$^{+/-}$ and D-HT postnatal day 7 (P7) mice. D-HT mice developed distorted tails by P7, whereas the others had normal tails, indicating genetic interaction between *Cfr* and *Fgf18*. (**C**) Alcian Blue/Alizarin Red staining of the tails of P7 mice. Tail distortion in D-HT mice was evident, whereas tails were normal in other genotypes. (**D**) Skeletons of compound mutant neonates. *Cfr*$^{+/-}$;*Fgf18*$^{+/-}$ double heterozygotes were crossed to generate compound mutants. Skeletons of wild-type, *Cfr*$^{-/-}$, *Cfr*$^{-/-}$;*Fgf18*$^{+/-}$, *Fgf18*$^{-/-}$, *Cfr*$^{+/-}$;*Fgf18*$^{-/-}$ and *Cfr*$^{-/-}$;*Fgf18*$^{-/-}$ neonates were stained with Alcian Blue and Alizarin Red. Top row, whole skeletons; lower row, ribs and spines from behind. As in Fig. 3C,D, *Cfr*$^{-/-}$ neonates showed tail distortion, and *Cfr*$^{-/-}$;*Fgf18*$^{+/-}$ neonates showed no obvious difference from *Cfr*$^{-/-}$ neonates. *Fgf18*$^{-/-}$ neonates showed slight distortion of the ribs, and *Cfr*$^{+/-}$;*Fgf18*$^{-/-}$ neonates showed enhanced distortion of the tail and curvature of the spine. In *Cfr*$^{-/-}$;*Fgf18*$^{-/-}$ double knockout neonates, the distortion of the ribs and curvature of the spine were much more severe than in *Cfr*$^{+/-}$;*Fgf18*$^{-/-}$ neonates. Scale bars: 2 mm in C and top row in D; 4 mm in lower row in D; 5 mm in B.

Physical interaction between Cfr and Fgf18, and enhancement of Fgf18-Fgfr3c signaling by Cfr

We examined the possibility that the genetic interaction of *Cfr* with *Fgf18* resulted from their physical interaction. To address this possibility, we prepared recombinant Fgf18 protein with a GST tag (GST-Fgf18), and used the GST tag alone as a control (Fig. 7A). We also prepared culture supernatant of COS7 cells transfected with an expression vector for the Cfr-EC. The purified GST-Fgf18 or GST tag was added to the supernatant, and Cfr-EC was immunoprecipitated. Western blot analysis revealed that GST-Fgf18 was co-immunoprecipitated with Cfr-EC, whereas the GST tag was not (Fig. 7B). These results clearly indicate that Fgf18 binds to Cfr and suggest that Cfr positively regulates Fgf18 signaling through this physical interaction.

To further confirm this possibility, we utilized a Ba/F3 cell line expressing Fgfr3c, which proliferates depending on Fgf18 (Ornitz et al., 1996). We chose Fgfr3c because it has the highest affinity for Fgf18 (Zhang et al., 2006) and is expressed in prehypertrophic chondrocytes in developing limb skeletons, where Cfr is also expressed (Ohbayashi et al., 2002) (Fig. 4). We infected these cells with viruses containing *Cfr* cDNA or without cDNA as a control, and assessed their responses to Fgf18 by WST-1 assay. Expression of Cfr enhanced the responses of Ba/F3 cells with Fgfr3c to Fgf18 (Fig. 6A), indicating that Cfr positively regulates Fgf18-Fgfr3c signaling. By contrast, Ba/F3 cells expressing Cfr alone failed to respond to Fgf18, whereas they proliferated in response to IL-3 (Fig. 6B). Based on these results, we concluded that Cfr enhances Fgf18 signaling via Fgfr3c but does not directly activate the intracellular signaling. As it is well known that heparin or HSPG is required for FGF signaling via FGFRs (Spivak-Kroizman et al., 1994; Yayon et al., 1991), we examined the effect of heparin on the Cfr function. We monitored responses of Ba/F3 cells expressing both Fgfr3c and Cfr to Fgf18 in the presence or absence of heparin and found that they failed to respond to Fgf18 at all in the absence of heparin, demonstrating that heparin is required for the function of Cfr (Fig. 6C).

Inhibition of the interaction between Cfr and Fgf18 by Dlk

The results described above demonstrate genetic, physical and functional interaction between Cfr and Fgf18. However, it still remained unknown how Dlk is involved in the interaction between Cfr and Fgf18.

As Cfr physically interacts with both Fgf18 and Dlk, we examined whether the binding of Dlk to Cfr affects the binding between Cfr and Fgf18. For this purpose, Cfr-EC was expressed in COS7 cells together with Dlk-Fc or CD4-Fc as a control. GST-Fgf18 fusion protein was then added to the culture supernatants and Cfr-EC was immunoprecipitated. Western blot analysis of the immunoprecipitates revealed that co-immunoprecipitation of Fgf18 with Cfr-EC was severely blocked in the presence of Dlk-Fc, but not CD4-Fc (Fig. 7C). These results indicate that Dlk interferes with the binding of Fgf18 to Cfr, resulting in interruption of the positive regulatory role of Cfr in Fgf18 signaling.

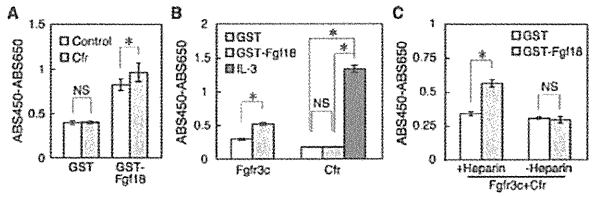

Fig. 6. Effects of Cfr in Fgf18 signaling in Ba/F3 cells. Ba/F3 cells were cultured in various conditions in 96 wells and the extent of proliferation was monitored by WST-1 assay. Absorbance at 450 nm subtracted by basal absorbance at 650 nm with s.d. is shown. We prepared eight wells for each condition. *P*-value was calculated with Student's *t*-test: *, $P<0.01$; NS, $P>0.2$. (**A**) Ba/F3 cells expressing Fgfr3c were infected with viruses carrying cDNA of *Cfr*, and we monitored proliferation in the presence of 500 ng/ml GST-Fgf18 or GST. As a control, Ba/F3 cells expressing Fgfr3c infected with viruses carrying no cDNA sequence were used. The cells with Cfr responded more strongly to Fgf18 than control cells. (**B**) Ba/F3 cells without FGFRs were infected with viruses carrying Cfr cDNA, and we monitored cell proliferation in the presence of 500 ng/ml GST-Fgf18 or GST, or 2 ng/ml IL-3. As a control for the activity of GST-Fgf18, we monitored responses of Ba/F3 cells with Fgfr3c to GST-Fgf18 at the same time. Ba/F3 cells with only Cfr could not respond to Fgf18, suggesting that Cfr does not directly activate the intracellular signaling. (**C**) Ba/F3 cells with both Fgfr3c and Cfr were activated by 500 ng/ml GST-Fgf18 in the presence or absence of 5 μg/ml heparin. The same concentration of GST was added as a control. The cells could not respond to Fgf18 in the absence of heparin.

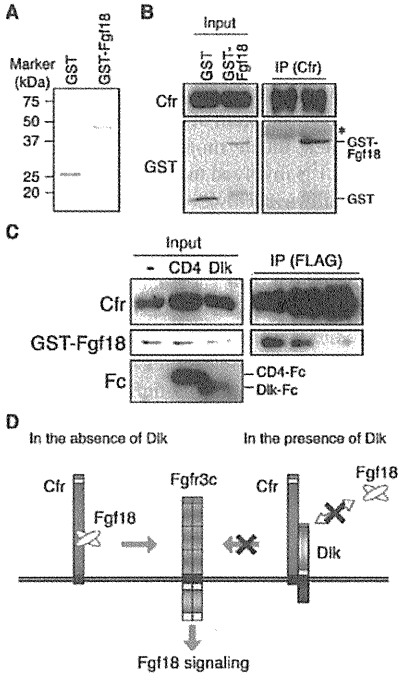

Fig. 7. The physical interaction between Cfr and Fgf18, and the effect of Dlk on that interaction. (**A**) Coomassie Brilliant Blue staining of GST and GST-Fgf18 purified from *E. coli*. (**B**) Interaction of Cfr with Fgf18. Cfr-EC was expressed in culture supernatant from COS7 cells, and GST-Fgf18 or GST was added to the supernatant. Then, Cfr-EC was precipitated with anti-Cfr serum and protein G Sepharose. GST-Fgf18, but not GST, was co-precipitated with Cfr-EC. *, non-specific band. (**C**) Interaction of Cfr with Fgf18 in the presence of Dlk. Cfr-EC together with Dlk-Fc or CD4-Fc were expressed in the culture supernatant from COS7 cells, and GST-Fgf18 was added to the supernatant. Then, FLAG-tagged Cfr-EC was precipitated with anti-FLAG M2 agarose. Dlk-Fc inhibited the interaction between Cfr and Fgf18, whereas CD4-Fc had no such effect. These results indicate that Dlk interrupts the physical interaction of Cfr with Fgf18. (**D**) A model of regulation of the Fgf18 signaling pathway by Cfr and Dlk. In the absence of Dlk, the extracellular domain of Cfr binds Fgf18 and positively regulates Fgf18 signaling. In the presence of Dlk, by contrast, Dlk binds to Cfr to inhibit the interaction between Cfr and Fgf18. Thus, the positive regulation of Fgf18 signaling by Cfr is disrupted by Dlk. Expression of Cfr and Dlk at the appropriate time modulates the strength of the signaling by Fgf18 and thereby contributes to normal developmental processes.

DISCUSSION

Cfr is a unique FGF-binding protein that binds FGFs via its long extracellular domain, but has a very short intracellular peptide of 13 amino acid residues without any known motifs for signaling. Therefore, it seems unlikely that Cfr directly activates the intracellular signaling pathways, which is in fact supported by the results using Ba/F3 cells expressing Cfr (Fig. 6B). Although Cfr seems to have no paralog in either mice or humans, it is evolutionally conserved and present even in *Caenorhabditis elegans* (data not shown), suggesting that Cfr is a fundamental component of the FGF signaling pathway. However, its physiological role remained unknown.

In this study we generated a *Cfr*-deficient mouse line and found that these mice exhibit perinatal lethality, growth retardation, distorted tails and cleft palates (Fig. 3). Another *Cfr*-deficient mouse line generated independently from this study shows the same phenotypes (H. Okae and Y. Iwakura, personal communication), supporting our results. Interestingly, among various *Fgf*-deficient mice reported so far, *Fgf18*-deficient mice exhibit phenotypes very similar to those of *Cfr*-deficient mice, such as perinatal death, growth retardation, tail distortion and cleft palate. Given this striking similarity, we considered that there is a functional link between Cfr and Fgf18. To address the genetic interaction of *Cfr* with *Fgf18*, double heterozygous mice were generated by mating $Cfr^{+/-}$ mice with $Fgf18^{+/-}$ mice. Although neither $Cfr^{+/-}$ nor $Fgf18^{+/-}$ mice showed any phenotype, the double heterozygous mice exhibited tail distortion after birth, suggesting genetic interaction (Fig. 5B,C). The phenotype is also strikingly similar to that of *Fgfr3*-deficient mice, which also exhibit tail distortion after birth (Deng et al., 1996). Because it has been well established that Fgf18 transmits its signal via Fgfr3c (Davidson et al., 2005), these observations further support the idea that Cfr is positively involved in Fgf18 signaling. Furthermore, co-immunoprecipitation assays clearly demonstrated that Cfr binds Fgf18 (Fig. 7B), and Ba/F3 cells expressing Fgfr3c with or without Cfr provided direct evidence for the positive regulatory role of Cfr in the Fgf18-Fgfr3c signaling pathway (Fig. 6A). This is the first report on the physiological functions of Cfr and the first evidence for the existence of a novel regulatory component of the Fgf18 signaling pathway. Fgfr3c is known to be expressed in proliferating and prehypertrophic chondrocytes to control their proliferation. Co-expression of Cfr with Fgfr3c in prehypertrophic chondrocytes supports the idea that Cfr plays a role in Fgfr3c signaling in those cells (Fig. 4). Because it has been well established that deregulation of the Fgf18-Fgfr3c signaling pathway leads to achondroplasia (Horton et al., 2007), it would be intriguing to investigate whether Cfr is also involved in human skeletal diseases.

Because Cfr has been shown to bind Fgf1, Fgf2, Fgf3 and Fgf4 (Burrus et al., 1992; Kohl et al., 2000), it may play a role in their signaling as well. In addition, the deletion of one *Cfr* allele in *Fgf18*-deficient mice augmented the skeletal abnormality of *Fgf18*-deficient mice and the deletion of both *Cfr* alleles in *Fgf18*-deficient mice resulted in a much more severe phenotype (Fig. 5D), suggesting that Cfr is involved in not only Fgf18 signaling but also other signaling pathways. However, as *Fgf4*-deficient mice die very early in their embryonic development (Feldman et al., 1995), and their phenotype is totally different from that of *Cfr*-deficient mice, Fgf4 is unlikely to be a physiological ligand for Cfr. By contrast, *Fgf3*-deficient mice show growth retardation and distorted tails, and some of them die perinatally similarly to *Cfr*-deficient mice, although their phenotypes are different from those of *Cfr*-deficient mice, e.g. inner ear defects in *Fgf3*-deficient mice (Mansour et al., 1993). Therefore, it is possible that Cfr contributes to Fgf3 signaling. Because *Fgf1*-deficient and *Fgf2*-deficient mice show rather mild phenotypes or no phenotype (Dono et al., 1998; Miller et al., 2000), it is hard to speculate about any possible involvement of Cfr in their signaling based on phenotypes. While there is currently no information as to the binding of Cfr to other FGFs, Cfr may contribute to signaling by some of them. In particular it would be interesting to investigate whether Cfr contributes to signaling by the FGFs that play a role in skeletal development, such as Fgf9 (Hung et al., 2007).

We identified Cfr as a Dlk-binding molecule (Fig. 1). Dlk is well known as preadipocyte factor 1 (Pref-1), an inhibitor of adipogenesis (Smas and Sul, 1993). In addition to preadipocytes, Dlk has also been reported to affect in vitro differentiation of various cell types such as osteoblasts (Abdallah et al., 2004), hematopoietic progenitors (Moore et al., 1997), thymocytes (Kaneta et al., 2000) and B-cell progenitors (Bauer et al., 1998). However, the mechanism by which Dlk functions still remains largely unknown. To reveal its functions, attempts were made to identify Dlk-binding molecules with the yeast two-hybrid system, resulting in several candidates such as growth arrest specific gene 1 (Baladron et al., 2002; Nueda et al., 2008). Because the extracellular domain of Dlk alone exerts its biological activities (Mei et al., 2002; Ohno et al., 2001; Smas et al., 1997), we used the extracellular domain of Dlk to search for its binding partners displayed on the cell surface and identified Cfr.

Because Dlk binds to Cfr, we investigated whether Dlk has any effect on the binding between Cfr and Fgf18 and revealed that Dlk blocks the binding (Fig. 7C). If the physical interaction of Cfr with Fgf18 is necessary for Cfr to positively regulate Fgf18 signaling, Dlk is likely to abrogate the positive role of Cfr in the signaling. We noticed that the phenotypes of *Cfr*-deficient mice are similar to those of *Dlk*-transgenic mice: e.g. both mice show growth retardation throughout their life and tail distortion (Lee et al., 2003). As loss of *Cfr* and forced expression of *Dlk* resulted in similar phenotypes, it is likely that Cfr and Dlk function in opposite ways. This is consistent with the result that Dlk inhibits the physical interaction between Cfr and Fgf18. Based on these results, we propose a model for the roles of Cfr and Dlk in Fgf18 signaling (Fig. 7D): i.e. in the absence of Dlk, binding of Cfr to Fgf18 positively regulates the signaling, and Dlk blocks the interaction between Cfr and Fgf18 by binding to Cfr, interrupting the positive regulatory role of Cfr in Fgf18 signaling. If this model is correct, the levels and timing of the expression of Cfr and Dlk would modulate Fgf18 signaling, fulfilling normal developmental processes. Recently, it was reported that Dlk regulates mesenchymal cell fate, such as chondrocyte, osteoblast and adipocyte lineages, through Sox9 (Wang and Sul, 2009). It is well known that Fgf18 also regulates chondrocyte and osteoblast development. Therefore, it is tempting to speculate that Fgf18 signaling is involved in the mechanism of cell-fate determination.

Recent studies have revealed that the FGF signaling via FGFRs is finely tuned by FGF-binding molecules other than FGFRs, such as HSPGs, Klothos and Fgfrl1 (Kurosu et al., 2007; Kurosu et al., 2006; Spivak-Kroizman et al., 1994; Suzuki et al., 2008b; Trueb et al., 2003; Urakawa et al., 2006). These molecules significantly contribute to normal developmental processes mediated by the FGF signaling pathways. This study has revealed, for the first time, in vivo roles of another FGF-binding molecule, Cfr, and unexpected links among Dlk, Cfr and FGF signaling, and provides evidence for the presence of a novel regulatory mechanism of the FGF signaling pathway.

Acknowledgements

We thank Drs T. Itoh, N. Tanimizu and E. Saijou, and Mr S. Saito for helpful discussions and technical assistance. We thank Ms K. Suzuki for preparing anti-Dlk antibody. We are also grateful to Drs A. Nakano, H. Okae, Y. Iwakura (the University of Tokyo), N. Mizushima, Y. Ogawa (Tokyo Medical and Dental University), J. Kanno, S. Kitajima, Y. Takahashi (National Institute of Health Science), N. Ohbayashi (Tohoku University) and T. Okubo (Okazaki Institute for Integrative Biosciences) for helpful advice and support. We thank Drs D. M. Ornitz (Washington University) and N. Iah (Kyoto University) for providing us with cDNAs of FGFRs and Fgf18, respectively. Y.M. is a recipient of a JSPS Research Fellowship for Young Scientists.

Supplementary material

Supplementary material for this article is available at http://dev.biologists.org/cgi/content/full/137/1/159/DC1

References

Abdallah, B. M., Jensen, C. H., Gutierrez, G., Leslie, R. G., Jensen, T. G. and Kassem, M. (2004). Regulation of human skeletal stem cells differentiation by Dlk1/Pref-1. *J. Bone Miner. Res.* **19**, 841-852.

Baertschi, S., Zhuang, L. and Trueb, B. (2007). Mice with a targeted disruption of the Fgfrl1 gene die at birth due to alterations in the diaphragm. *FEBS J.* **274**, 6241-6253.

Baladron, V., Ruiz-Hidalgo, M. J., Bonvini, E., Gubina, E., Notario, V. and Laborda, J. (2002). The EGF-like homeotic protein dlk affects cell growth and interacts with growth-modulating molecules in the yeast two-hybrid system. *Biochem. Biophys. Res. Commun.* **291**, 193-204.

Bauer, S. R., Ruiz-Hidalgo, M. J., Rudikoff, E. K., Goldstein, J. and Laborda, J. (1998). Modulated expression of the epidermal growth factor-like homeotic protein dlk influences stromal-cell-pre-B-cell interactions, stromal cell adipogenesis, and pre-B-cell interleukin-7 requirements. *Mol. Cell. Biol.* **18**, 5247-5255.

Burrus, L. W. and Olwin, B. B. (1989). Isolation of a receptor for acidic and basic fibroblast growth factor from embryonic chick. *J. Biol. Chem.* **264**, 18647-18653.

Burrus, L. W., Zuber, M. E., Lueddecke, B. A. and Olwin, B. B. (1992). Identification of a cysteine-rich receptor for fibroblast growth factors. *Mol. Cell. Biol.* **12**, 5600-5609.

Davidson, D., Blanc, A., Filion, D., Wang, H., Plut, P., Pfeffer, G., Buschmann, M. D. and Henderson, J. E. (2005). Fibroblast growth factor (FGF) 18 signals through FGF receptor 3 to promote chondrogenesis. *J. Biol. Chem.* **280**, 20509-20515.

Deng, C., Wynshaw-Boris, A., Zhou, F., Kuo, A. and Leder, P. (1996). Fibroblast growth factor receptor 3 is a negative regulator of bone growth. *Cell* **84**, 911-921.

Dono, R., Texido, G., Dussel, R., Ehmke, H. and Zeller, R. (1998). Impaired cerebral cortex development and blood pressure regulation in FGF-2-deficient mice. *EMBO J.* **17**, 4213-4225.

Eswarakumar, V. P., Lax, I. and Schlessinger, J. (2005). Cellular signaling by fibroblast growth factor receptors. *Cytokine Growth Factor Rev.* **16**, 139-149.

Feldman, B., Poueymirou, W., Papaioannou, V. E., DeChiara, T. M. and Goldfarb, M. (1995). Requirement of FGF-4 for postimplantation mouse development. *Science* **267**, 246-249.

Haque, T., Nakada, S. and Hamdy, R. C. (2007). A review of FGF18: its expression, signaling pathways and possible functions during embryogenesis and post-natal development. *Histol. Histopathol.* **22**, 97-105.

Horton, W. A., Hall, J. G. and Hecht, J. T. (2007). Achondroplasia. *Lancet* **370**, 162-172.

Hung, I. H., Yu, K., Lavine, K. J. and Ornitz, D. M. (2007). FGF9 regulates early hypertrophic chondrocyte differentiation and skeletal vascularization in the developing stylopod. *Dev. Biol.* **307**, 300-313.
Kaneta, M., Osawa, M., Sudo, K., Nakauchi, H., Farr, A. G. and Takahama, Y. (2000). A role for pref-1 and HES-1 in thymocyte development. *J. Immunol.* **164**, 256-264.
Kohl, R., Antoine, M., Olwin, B. B., Dickson, C. and Kiefer, P. (2000). Cysteine-rich fibroblast growth factor receptor alters secretion and intracellular routing of fibroblast growth factor 3. *J. Biol. Chem.* **275**, 15741-15748.
Kurosu, H., Ogawa, Y., Miyoshi, M., Yamamoto, M., Nandi, A., Rosenblatt, K. P., Baum, M. G., Schiavi, S., Hu, M. C., Moe, O. W. et al. (2006). Regulation of fibroblast growth factor-23 signaling by klotho. *J. Biol. Chem.* **281**, 6120-6123.
Kurosu, H., Choi, M., Ogawa, Y., Dickson, A. S., Goetz, R., Eliseenkova, A. V., Mohammadi, M., Rosenblatt, K. P., Kliewer, S. A. and Kuro-o, M. (2007). Tissue-specific expression of betaKlotho and fibroblast growth factor (FGF) receptor isoforms determines metabolic activity of FGF19 and FGF21. *J. Biol. Chem.* **282**, 26687-26695.
Lee, K., Villena, J. A., Moon, Y. S., Kim, K. H., Lee, S., Kang, C. and Sul, H. S. (2003). Inhibition of adipogenesis and development of glucose intolerance by soluble preadipocyte factor-1 (Pref-1). *J. Clin. Invest.* **111**, 453-461.
Liu, Z., Xu, J., Colvin, J. S. and Ornitz, D. M. (2002). Coordination of chondrogenesis and osteogenesis by fibroblast growth factor 18. *Genes Dev.* **16**, 859-869.
Mansour, S. L., Goddard, J. M. and Capecchi, M. R. (1993). Mice homozygous for a targeted disruption of the proto-oncogene int-2 have developmental defects in the tail and inner ear. *Development* **117**, 13-28.
Mei, B., Zhao, L., Chen, L. and Sul, H. S. (2002). Only the large soluble form of preadipocyte factor-1 (Pref-1), but not the small soluble and membrane forms, inhibits adipocyte differentiation: role of alternative splicing. *Biochem. J.* **364**, 137-144.
Miller, D. L., Ortega, S., Bashayan, O., Basch, R. and Basilico, C. (2000). Compensation by fibroblast growth factor 1 (FGF1) does not account for the mild phenotypic defects observed in FGF2 null mice. *Mol. Cell. Biol.* **20**, 2260-2268.
Miyaoka, Y., Tanaka, M., Naiki, T. and Miyajima, A. (2006). Oncostatin M inhibits adipogenesis through the RAS/ERK and STAT5 signaling pathways. *J. Biol. Chem.* **281**, 37913-37920.
Moon, Y. S., Smas, C. M., Lee, K., Villena, J. A., Kim, K. H., Yun, E. J. and Sul, H. S. (2002). Mice lacking paternally expressed Pref-1/Dlk1 display growth retardation and accelerated adiposity. *Mol. Cell. Biol.* **22**, 5585-5592.
Moore, K. A., Pytowski, B., Witte, L., Hicklin, D. and Lemischka, I. R. (1997). Hematopoietic activity of a stromal cell transmembrane protein containing epidermal growth factor-like repeat motifs. *Proc. Natl. Acad. Sci. USA* **94**, 4011-4016.
Nueda, M. L., Garcia-Ramirez, J. J., Laborda, J. and Baladron, V. (2008). dlk1 specifically interacts with insulin-like growth factor binding protein 1 to modulate adipogenesis of 3T3-L1 cells. *J. Mol. Biol.* **379**, 428-442.
Ohbayashi, N., Shibayama, M., Kurotaki, Y., Imanishi, M., Fujimori, T., Itoh, N. and Takada, S. (2002). FGF18 is required for normal cell proliferation and differentiation during osteogenesis and chondrogenesis. *Genes Dev.* **16**, 870-879.
Ohno, N., Izawa, A., Hattori, M., Kageyama, R. and Sudo, T. (2001). dlk inhibits stem cell factor-induced colony formation of murine hematopoietic progenitors: Hes-1-independent effect. *Stem Cells* **19**, 71-79.
Ornitz, D. M., Xu, J., Colvin, J. S., McEwen, D. G., MacArthur, C. A., Coulier, F., Gao, G. and Goldfarb, M. (1996). Receptor specificity of the fibroblast growth factor family. *J. Biol. Chem.* **271**, 15292-15297.
Raghunandan, R., Ruiz-Hidalgo, M., Jia, Y., Ettinger, R., Rudikoff, E., Riggins, P., Farnsworth, R., Tesfaye, A., Laborda, J. and Bauer, S. R. (2008). Dlk1 influences differentiation and function of B lymphocytes. *Stem Cells Dev.* **17**, 495-507.
Smas, C. M. and Sul, H. S. (1993). Pref-1, a protein containing EGF-like repeats, inhibits adipocyte differentiation. *Cell* **73**, 725-734.
Smas, C. M., Chen, L. and Sul, H. S. (1997). Cleavage of membrane-associated pref-1 generates a soluble inhibitor of adipocyte differentiation. *Mol. Cell. Biol.* **17**, 977-988.
Spivak-Kroizman, T., Lemmon, M. A., Dikic, I., Ladbury, J. E., Pinchasi, D., Huang, J., Jaye, M., Crumley, G., Schlessinger, J. and Lax, I. (1994). Heparin-induced oligomerization of FGF molecules is responsible for FGF receptor dimerization, activation, and cell proliferation. *Cell* **79**, 1015-1024.
Suzuki, K., Tanaka, M., Watanabe, N., Saito, S., Nonaka, H. and Miyajima, A. (2008a). p75 Neurotrophin receptor is a marker for precursors of stellate cells and portal fibroblasts in mouse fetal liver. *Gastroenterology* **135**, 270-281 e3.
Suzuki, M., Uehara, Y., Motomura-Matsuzaka, K., Oki, J., Koyama, Y., Kimura, M., Asada, M., Komi-Kuramochi, A., Oka, S. and Imamura, T. (2008b). betaKlotho is required for fibroblast growth factor (FGF) 21 signaling through FGF receptor (FGFR) 1c and FGFR3c. *Mol. Endocrinol.* **22**, 1006-1014.
Tanimizu, N., Nishikawa, M., Saito, H., Tsujimura, T. and Miyajima, A. (2003). Isolation of hepatoblasts based on the expression of Dlk/Pref-1. *J. Cell Sci.* **116**, 1775-1786.
Tanimizu, N., Saito, H., Mostov, K. and Miyajima, A. (2004). Long-term culture of hepatic progenitors derived from mouse Dlk+ hepatoblasts. *J. Cell Sci.* **117**, 6425-6434.
Trueb, B., Zhuang, L., Taeschler, S. and Wiedemann, M. (2003). Characterization of FGFRL1, a novel fibroblast growth factor (FGF) receptor preferentially expressed in skeletal tissues. *J. Biol. Chem.* **278**, 33857-33865.
Urakawa, I., Yamazaki, Y., Shimada, T., Iijima, K., Hasegawa, H., Okawa, K., Fujita, T., Fukumoto, S. and Yamashita, T. (2006). Klotho converts canonical FGF receptor into a specific receptor for FGF23. *Nature* **444**, 770-774.
Wang, Y. and Sul, H. S. (2009). Pref-1 regulates mesenchymal cell commitment and differentiation through Sox9. *Cell Metab.* **9**, 287-302.
Wiedemann, M. and Trueb, B. (2000). Characterization of a novel protein (FGFRL1) from human cartilage related to FGF receptors. *Genomics* **69**, 275-279.
Yayon, A., Klagsbrun, M., Esko, J. D., Leder, P. and Ornitz, D. M. (1991). Cell surface, heparin-like molecules are required for binding of basic fibroblast growth factor to its high affinity receptor. *Cell* **64**, 841-848.
Zhang, X., Ibrahimi, O. A., Olsen, S. K., Umemori, H., Mohammadi, M. and Ornitz, D. M. (2006). Receptor specificity of the fibroblast growth factor family: the complete mammalian FGF family. *J. Biol. Chem.* **281**, 15694-15700.
Zhou, Z., Zuber, M. E., Burrus, L. W. and Olwin, B. B. (1997). Identification and characterization of a fibroblast growth factor (FGF) binding domain in the cysteine-rich FGF receptor. *J. Biol. Chem.* **272**, 5167-5174.

GASTROENTEROLOGY 2010;138:1525–1535

BASIC—LIVER, PANCREAS, AND BILIARY TRACT

Characterization and Functional Analyses of Hepatic Mesothelial Cells in Mouse Liver Development

IZUMI ONITSUKA,* MINORU TANAKA,*,‡ AND ATSUSHI MIYAJIMA*

*Laboratory of Cell Growth and Differentiation and ‡Promotion of Independence for Young Investigators, Institute of Molecular and Cellular Biosciences, University of Tokyo, Tokyo, Japan

BACKGROUND & AIMS: At the onset of liver development, cardiac mesoderm, septum transversum mesenchyme, and endothelial cells are involved in the specification and/or proliferation of hepatoblasts. After this initial stage, however, it is unclear which cells support the proliferation and differentiation of hepatocytes. Here we characterized the nature of mouse hepatic mesothelial cells (MCs) and investigated their role in organogenesis. **METHODS:** Using anti-podocalyxin-like protein 1 (PCLP1) and anti-mesothelin antibodies, we characterized MCs during liver development by immunohistochemistry, flow cytometry, and gene expression analysis. The possible role of MCs in hepatogenesis was investigated by in vitro culture and analysis of Wilms' tumor 1 homologue (WT1) knockout mice. **RESULTS:** PCLP1 was highly expressed in immature MCs, covering the surface of lobes. PCLP1 expression in MCs was down-regulated along with development, whereas mesothelin expression was up-regulated, indicating that these molecules distinguished developmental stages of MCs. The proliferation potential of MCs was high in the fetus and declined after birth. Fetal MCs expressed various growth factors and strongly enhanced the expansion of fetal hepatocytes in vitro, whereas differentiated MCs exhibited less growth factor expression, and differentiated MCs failed to enhance hepatocyte proliferation in vitro. In WT1-deficient embryos, hepatocyte proliferation was impaired due to defective MCs. **CONCLUSIONS: The mesothelium is not only an inert protective sheet covering the parenchyma but also changes its characteristics dynamically during development and plays an active role in organogenesis by promoting expansion of parenchymal cells.**

Keywords: Mesothelium; Mesothelin; Podocalyxin-Like Protein 1; Cell Sorting.

In mouse liver development, hepatic cells are induced from the embryonic endoderm by embryonic day (E) 8.5. The cardiac mesoderm and septum transversum mesenchyme (STM) adjacent to the foregut endoderm produce fibroblast growth factors and bone morphogenetic protein, respectively, to induce liver specification.[1,2] Thereafter, the specified endodermal cells, hepatoblasts, outgrow into the STM to form hepatic cords by the support of endothelial cells (ECs).[3] However, the mechanism of liver development after the liver bud formation remains largely unknown. Although various cytokines have been shown to stimulate proliferation of hepatocytes in vitro (eg, epidermal growth factor, hepatocyte growth factor [HGF], and pleiotrophin [Ptn]),[4,5] it remains elusive how hepatocyte proliferation is supported by surrounding cells in vivo. The lack of tools to precisely identify and isolate different types of liver cells has hampered such investigation. Suksaweang et al have shown that proliferation of hepatocytes is limited to the peripheral region of the hepatic lobe during liver development in the chick.[6] They also suggested that mesenchymal cells located at the periphery of the lobe might provide the microenvironment for hepatocytes to proliferate.[6] However, it was unclear which peripheral mesenchymal cells contribute to hepatogenesis during liver development.

In vertebrates, the periphery of all coelomic organs is covered by a single layer of mesothelial tissue, which provides nonadhesive and protective surfaces. The mesothelium is derived from the lateral plate mesoderm and is believed to play an important role in maintaining normal serosal integrity and functions, such as transport

Abbreviations used in this paper: Ab, antibody; bFGF, basic fibroblast growth factor; Dlk1, delta-like 1 homologue; E, embryonic day; EC, endothelial cell; HGF, hepatocyte growth factor; IHC, immunohistochemistry; MC, mesothelial cell; Mdk, midkine; Msln, mesothelin; OSM, oncostatin M; PCLP1, podocalyxin-like protein 1; PCR, polymerase chain reaction; PD, postnatal day; Ptn, pleiotrophin; RALDH2, retinaldehyde dehydrogenase; RT, reverse-transcription; STM, septum transversum mesenchyme; WT1, Wilms' tumor 1 homologue.

0016-5085/10/$36.00
doi:10.1053/j.gastro.2009.12.059

of fluid and cells in serosal cavities, antigen presentation, inflammation, and tissue repair.[7] During vertebrate development, recent studies have shown that splanchnic mesothelial cells (MCs) delaminate into the parenchymal region and give rise to the vascular cells and mesenchymal cells in multiple coelomic organs, including murine heart,[8] lung,[9] gut,[10] and avian liver.[11] These observations suggest that splanchnic MCs might play important roles in organogenesis as a source of vascular and/or mesenchymal cells in multiple organs. Despite these accumulating reports, however, the precise characteristics of MCs and their roles for the development of parenchymal cells remain largely unknown.

In this study, we show that podocalyxin-like protein 1 (PCLP1) and mesothelin (Msln) are excellent markers to identify and isolate hepatic MCs. PCLP1 is a member of the sialomucin family and was originally identified as a protein highly expressed on glomerular podocytes in avian and mammalian kidneys.[12] It was also reported that PCLP1 is expressed on ECs,[13] immature mesodermal cells such as hemangioblasts, the common progenitor for hematopoietic and vascular endothelial cells,[14] and hematopoietic stem cells.[15] Msln is a glycosylphosphatidylinositol-linked glycoprotein highly expressed in a variety of normal mesothelial tissues, mesotheliomas, and ovarian cancers.[16] Using these cell surface markers, we characterize MCs and show that fetal hepatic MCs are a rich source of multiple growth factors for hepatocytes from early to late stages in liver development, indicating that MC layers play an active role in organogenesis.

BASIC—LIVER, PANCREAS, AND BILIARY TRACT

Materials and Methods

Mice

C57BL/6 mice were purchased from Nihon SLC (Hamamatsu, Japan). Mice were maintained and mated in the institutional animal facility according to the guidelines of the University of Tokyo. The time at midday (12:00) was taken to be E0.5 for plugged mice. WT1 knockout mice[17] were kindly provided by Dr R. Nishinakamura. Embryos were genotyped by polymerase chain reaction (PCR).

Cell Preparation for Flow Cytometric Analysis and Sorting

Livers isolated from embryos were dissociated into a single-cell suspension and stained by antibodies according to the previous report.[18] Cells were analyzed by FACSCalibur (BD Biosciences) or EPICS ALTRA (Beckman Coulter, San Diego, CA). For cell sorting, EPICS ALTRA or autoMACS (Miltenyi Biotec K.K., Tokyo, Japan) instruments were used. Purity of the sorted cell populations estimated by flow cytometry was higher than 90%.

Expansion of Fetal Hepatic MCs and Coculture With Hepatoblasts

Flk1^{-}PCLP1^{high} cells were sorted from E12.5 livers by a cell sorter and expanded in vitro on type IV collagen-coated dishes in α-minimum essential medium containing 10% fetal bovine serum and 50 nmol/L mercaptoethanol, 10 ng/mL oncostatin M (OSM), and 10 ng/mL basic fibroblast growth factor (bFGF). For passage, cells were trypsinized with 0.05% trypsin and 0.5 mmol/L EDTA (Sigma-Aldrich, St. Louis, MO) in phosphate-buffered saline at 37°C for 8 minutes and replated. Delta-like 1 homologue (Dlk1^{+}) fetal hepatoblasts were purified from E14.5 livers using autoMACS as reported previously. A total of 2×10^3 Dlk1^{+} cells were inoculated into each well of a gelatin-coated 24-well plate with α-minimum essential medium containing 10% fetal bovine serum with or without 1×10^5 in vitro expanded fetal hepatic MCs, which were separated in a 3.0-μm pored Transwell (Corning, NY). As a positive control for proliferation, 25 ng/mL pleiotrophin (Ptn) or 50 ng/mL midkine (Mdk) was added to the culture. After 3 days of culture, cells were stained with Giemsa solution to visualize the colonies or subjected to WST-1 assay (Roche, Diagnostics KK, Tokyo, Japan) according to the manufacturer's protocol. Averages in triplicate cultures were used to determine cell proliferation.

Results

PCLP1 Is Highly Expressed on the Surface Layers of Multiple Coelomic Organs During Embryogenesis

It was reported previously that PCLP1 is widely expressed by "boundary elements," including vasculature, mesothelial linings, and the luminal surface of newly formed cavities in murine embryos.[15] Immunohistochemistry (IHC) of embryonic sections with anti-PCLP1 antibody (Ab) showed that PCLP1 was expressed highly on the surface of multiple coelomic organs such as heart, lung, liver, and stomach (data not shown). Because all the coelomic organs are covered by a single layer of MCs, cells with an intense PCLP1 signal were suggested to be the mesothelial lining.

On E9.5 tissue sections, double staining with anti-PCLP1 Ab and anti-Dlk1 Ab, which recognizes fetal hepatoblasts,[18,19] showed the presence of PCLP1^{+} cells in the STM, where hepatic cords form with Dlk1^{+} hepatoblasts emerging from the foregut endoderm (Figure 1*A*). At E10.5, a monolayer of cells with an intense PCLP1 signal was detected on the surfaces of dorsal lobes, and these cells covered each hepatic lobe completely at E12.5 (Figure 1*A*). While the signals were continuously detected at E16.5, their frequency and intensity were reduced at postnatal day (PD) 4, and no PCLP1 signal was detected on the surface of adult livers (Figure 1*A*). These results suggested that the PCLP1 expression on the surface of hepatic lobes is regulated in a stage-specific manner. By

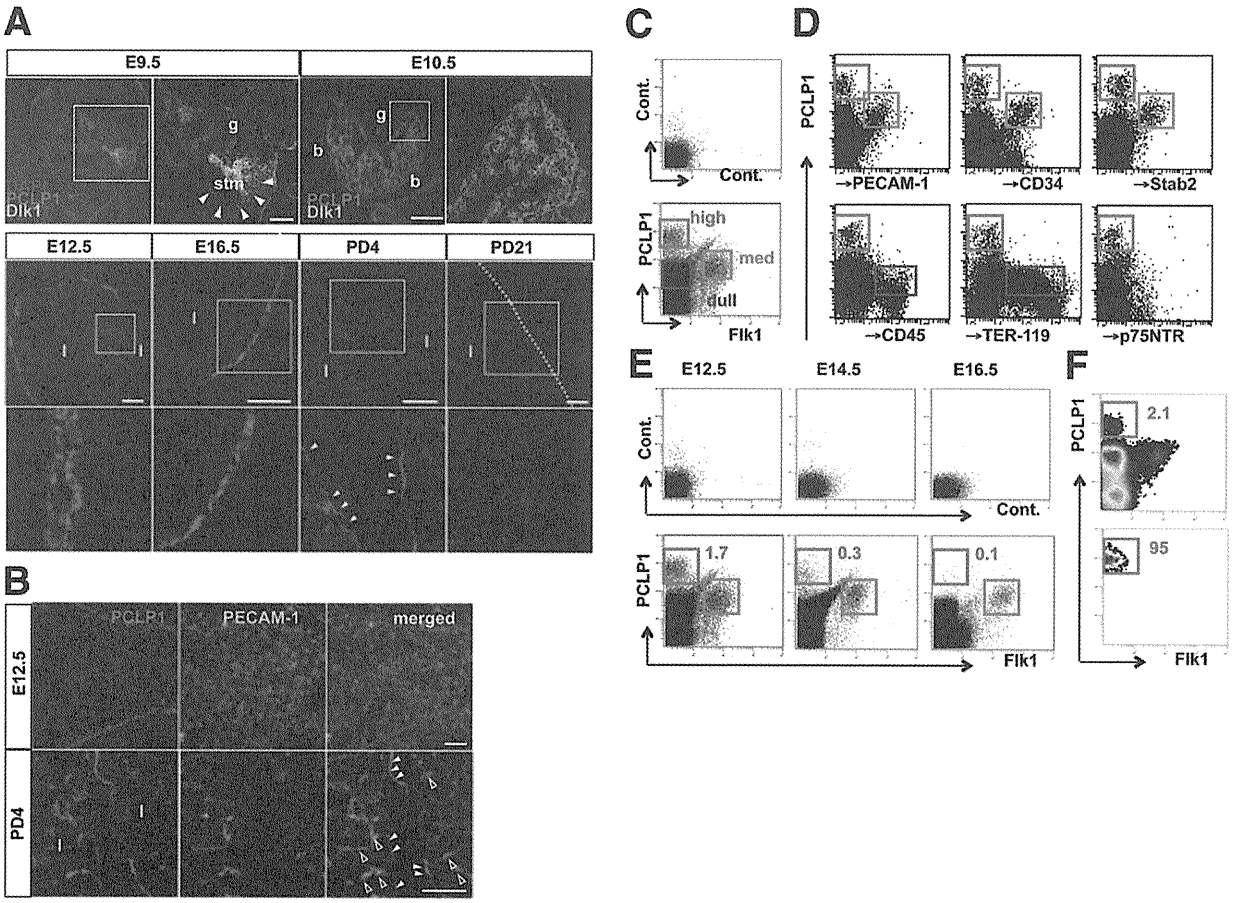

Figure 1. IHC and flow cytometry with anti-PCLP1 Ab in the developing liver. (*A* and *B*) IHC with anti-PCLP1 (*red*), anti-Dlk1 (*green* in *A*), and anti–PECAM-1 (*green* in *B*) Abs and 4′,6-diamidino-2-phenylindole (*blue* in *A*). Higher-magnification images of the *boxed regions* in *A* are shown to the right (E9.5 and E10.5) or underneath (E12.5 to PD21). The *dotted line* in *A* (PD21) delineates the periphery of the hepatic lobe. *Arrowheads* indicate PCLP1$^+$ cells in the STM region (E9.5) or in the mesothelial layer (PD4 in *A* and *B*), respectively. *Open arrowheads* in *B* indicate PECAM1$^+$PCLP1^{med} sinusoidal ECs. g, gut; stm, septum transversum mesenchyme; b, body wall; l, lobe. *Scale bars* = 100 μm. (*C*) Flow cytometry of E12.5 liver cells using anti-PCLP1 and anti-Flk1 Abs. *Red*, *green*, and *blue lines* in the *lower panel* indicate Flk1$^-$PCLP1^{high}, Flk1$^+$PCLP1^{med}, and Flk1$^-$PCLP1^{dull} cell populations, respectively. (*D*) Flow cytometry of E12.5 liver cells using anti-PCLP1 Ab and other cell surface molecules. *Red*, *green*, and *blue lines* in each *panel* indicate PCLP1^{high}, PCLP1^{med}, and PCLP1^{dull} cell populations, respectively. (*E*) Flow cytometry of E12.5, E14.5, and E16.5 liver cells using anti-PCLP1 and anti-Flk1 Abs. *Red* and *green lines* in each *lower panel* indicate Flk1$^-$PCLP1^{high} and Flk1$^+$PCLP1^{med} cells, respectively. The number indicates the percentage of Flk1$^-$PCLP1^{high} cells. (*F*) Flow cytometry of E12.5 liver cells before (*upper panel*) and after (*lower panel*) sorting of Flk1$^-$PLCP1^{high} cells by a cell sorter. Sorting gates are indicated by *red lines*. Numbers in each *panel* indicate the percentage of Flk1$^-$PCLP1^{high} cells.

contrast, weak PCLP1 signals were observed in the parenchymal region from E12.5 to adults. In accordance with the previous report that PCLP1 is expressed on ECs,[13] weak PCLP1 signals colocalized with PECAM-1, an endothelial marker, in the parenchymal region; however, no colocalization occurred with strong PCLP1 signals in the mesothelial lining (Figure 1*B*).

Flow Cytometric Analysis of PCLP1$^+$ Cells in Fetal Liver

Flow cytometry of E12.5 fetal liver cells with anti-PCLP1 Ab and anti-Flk1 Ab, which detects ECs, revealed that PCLP1$^+$ cells could be fractionated into at least 3 populations, PCLP1^{high}, PCLP1^{med}, and PCLP1^{dull} cells, based on the expression levels of PCLP1 (Figure 1*C*). Multicolor flow cytometry revealed that PCLP1^{med} cells were positive for several EC markers but not for CD45 (Figure 1*D* and data not shown). PCLP1^{dull} cells contained TER-119$^+$ erythroids and CD45$^+$ leukocytes (Figure 1*D*), consistent with the previous report.[15] By contrast, PCLP1^{high} cells were completely negative for EC and blood cell markers as well as the hepatic stellate cell marker p75 neurotrophin receptor[20] (Figure 1*C*–*E*), indicating that the Flk1$^-$PCLP1^{high} cell population was distinct from these nonparenchymal cells. The fraction of Flk1$^-$PCLP1^{high} cells in total fetal liver cells decreased as development progressed (Figure 1*E*).

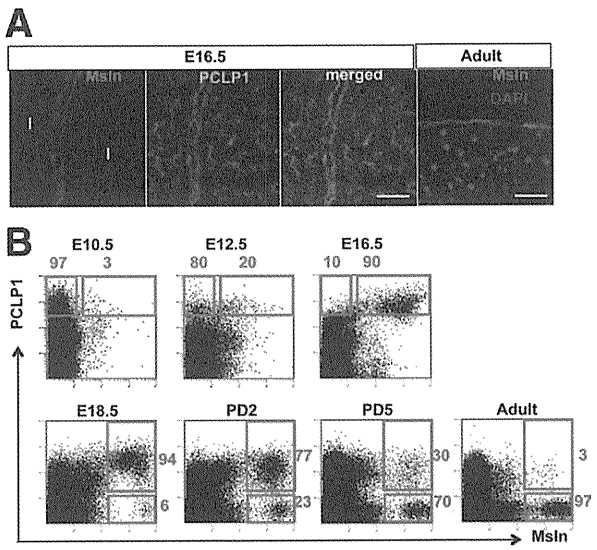

Figure 2. Expression of PCLP1 and Msln in the mesothelial layer during liver development. (*A*) IHC of liver sections with anti-Msln (*red*) and anti-PCLP1 (*green*) Abs. l, lobe. *Scale bars* = 80 μm. (*B*) Flow cytometry of liver cells with anti-PCLP1 and anti-Msln Abs. *Red lines* in each panel indicate PCLP1^{high} (*upper panels*) and Msln^{+} (*lower panels*) cell populations, respectively. The cells of whole livers (E10.5 and E12.5) and surgically separated mesothelial tissues (E16.5, E18.5, PD2, PD5, and Adult) were used for flow cytometry. Numbers in each *panel* indicate the percentage of each cell population in PCLP1^{high} (*upper panels*) or in Msln^{+} (*lower panels*) cells.

Flow cytometry of surgically separated E16.5 livers into mesothelial and nonmesothelial tissues under a stereomicroscope revealed that Flk1^{-}PCLP1^{high} cells were present exclusively in the mesothelial tissue, while Flk1^{+}PCLP1^{med} cells were detected mainly in the nonmesothelial tissue (Supplementary Figure 1*A* and *B*). These results indicated that the PCLP1^{high} and PCLP1^{med} cells by flow cytometry correspond to fetal MCs and ECs detected by IHC, respectively, and that PCLP1^{high} cells could be isolated by a cell sorter with high purity (Figure 1*F*).

Expression of PCLP1 and Msln in Hepatic MCs During Liver Development

Msln is known to be a general marker for MCs. IHC showed that a single cell layer of mesothelial lining was specifically stained by both anti-Msln and anti-PCLP1 Abs in E16.5 liver sections (Figure 2*A*). In contrast to the lack of PCLP1 expression in adult MCs (Figure 1*A*), Msln was strongly expressed on adult MCs (Figure 2*A*) but not on fetal livers at earlier stages (data not shown). Cells highly expressing Msln were exclusively detected by flow cytometry in the surgically separated mesothelial tissue in PD0 and adult livers (Supplementary Figure 1*C*). These results suggested that MCs changed surface phenotypes from PCLP1^{+} to Msln^{+} during development. Consistent with the results of IHC, flow cytometry clearly showed that most of the PCLP1^{high} cells were Msln^{-} in E10.5 liver cell suspensions (Figure 2*B*). Interestingly, the fraction of Msln^{+} cells in the PCLP1^{high} cell population increased as fetal development progressed, while PCLP1^{+} cells in the Msln^{+} population decreased gradually after birth (Figure 2*B*). These results indicated that the expression of PCLP1 and Msln is developmentally regulated, and 3 developmental stages of MCs can be distinguished based on the expression of these 2 markers, that is, PCLP1^{high}Msln^{-}, PCLP1^{+}Msln^{+}, and PCLP1^{-}Msln^{+} MCs are the immature, intermediate, and mature stages of MCs, respectively.

Development of an In Vitro Culture System for Fetal MCs

To further characterize fetal MCs, we have developed an in vitro culture system for fetal MCs isolated by a cell sorter based on the expression of PCLP1 and/or Msln. The proliferation potential of MCs was determined by in vitro colony formation assay (see Supplementary Materials and Methods). Total numbers of colonies formed from 1 × 10^3 MCs isolated from E12.5, E18.5, and PD7 livers were 251.0 ± 5.7, 229.7 ± 19.7, and 95.3 ± 7.1, respectively, indicating that fetal hepatic MCs possessed higher proliferation potential than postnatal MCs. Adult hepatic MCs formed very few colonies (~3/1000 MCs; Figure 3*A* and *B*). Only PCLP1^{+}Msln^{+} MCs formed large colonies consisting of more than 300 cells, whereas the size of colonies formed from PD7 MCs was small (Figure 3*A* and *B*), indicating that hepatic MCs at the intermediate stage proliferate most actively and the proliferation potential of hepatic MCs declines after birth.

Interestingly, the cultivation of E12.5 PCLP1^{high}Msln^{-} cells changed the expression of PCLP1 and Msln, similar to the developmental change in vivo as shown in Figure 2*B* (Figure 3*C*). In this culture condition without exogenous cytokines, fetal MCs proliferated modestly but their proliferation ceased within several days. Additionally, they became PCLP1^{-}Msln^{+} MCs, a phenotype similar to adult MCs (Figure 3*C* and *D*). We found that addition of OSM and bFGF to culture medium synergistically promoted the expansion of fetal MCs (Figure 3*D*). Furthermore, 49% of the E12.5 PCLP1^{high} MCs maintained expression of PCLP1 after 6 days of cultivation in the presence of OSM and bFGF, while only 8% of the cells did so in their absence (Figure 3*E*). The continuous presence of OSM and bFGF in the culture medium maintained the expression of PCLP1 after the first passage, while their removal resulted in rapid down-regulation of PCLP1 expression and up-regulation of Msln expression (Figure 3*F* and Supplementary Figure 2). These results strongly suggested that OSM and bFGF could maintain immature characteristics of fetal MCs, whereas MCs proceeded to differentiate without them.

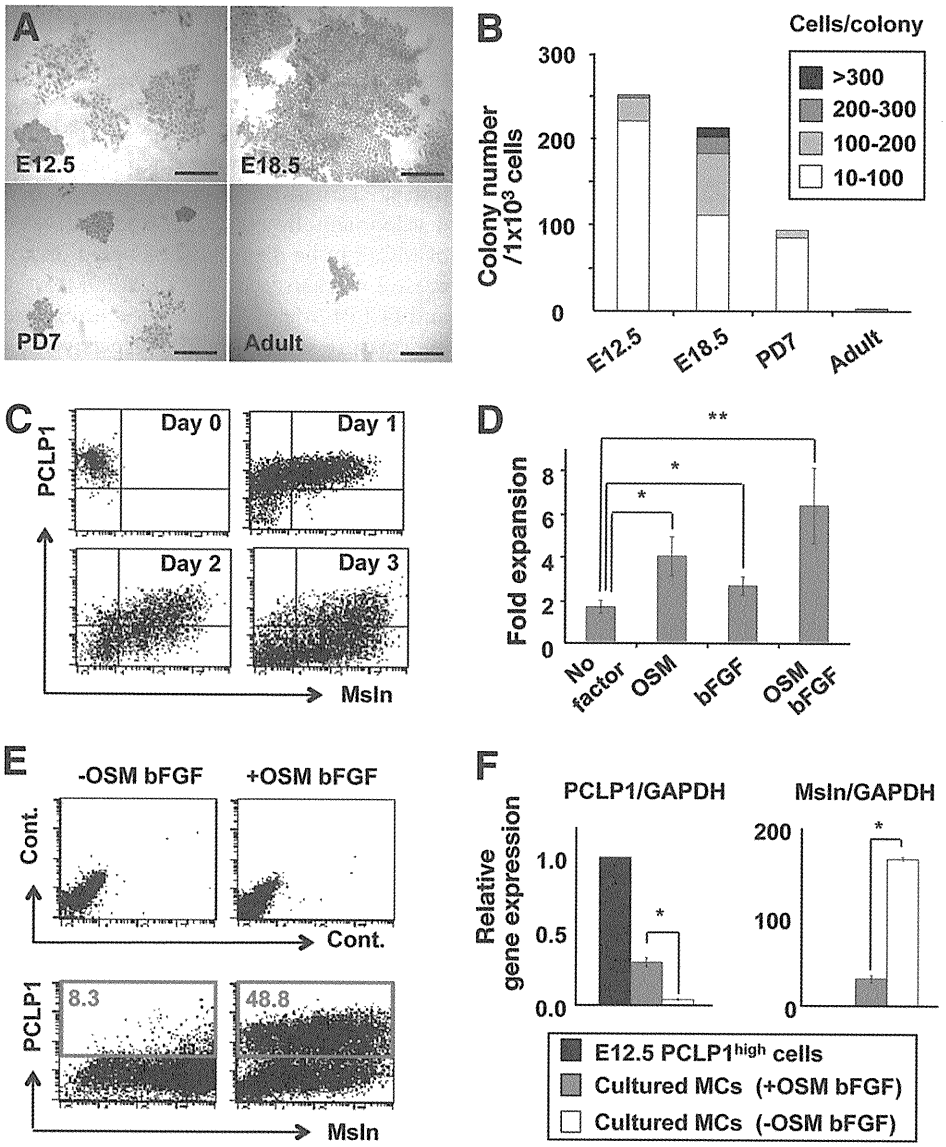

Figure 3. Expansion and differentiation of fetal MCs in vitro. (*A*) Colony-forming activity of hepatic MCs isolated from various stages of developing liver. Morphology of colonies formed from immature (E12.5), intermediate (E18.5), or mature (PD7 and Adult) MCs are shown. Colonies were stained with Giemsa solution after 6 days in culture. *Scale bars* = 80 μm. (*B*) Quantification of colony-forming potentials of MCs isolated from E12.5, E18.5, PD7, or adult liver. Averages of 3 wells for each sample are indicated. (*C*) Flow cytometry of cultured PCLP1^{high}Msln^{-} cells. Sorted cells from E12.5 liver were incubated and stained with anti-PCLP1 and anti-Msln Abs at the indicated time points. (*D*) Proliferation of fetal MCs in vitro. Flk1^{-}PCLP1^{high} cells sorted from E12.5 livers were cultured in the presence or absence of cytokines (10 ng/mL each) as indicated, and cell numbers were determined at day 6. Averages of 3 wells for each sample are shown. $^{*}P < .05$, $^{**}P < .01$; Student *t* test. (*E*) Flow cytometry of cultured MCs with anti-PCLP1 and anti-Msln Abs. Freshly isolated E12.5 Flk1^{-}PCLP1^{high} cells were cultured for 6 days in the presence or absence of OSM and bFGF and analyzed by flow cytometry. *Red lines* and *numbers* in the *lower panels* indicate PCLP1^{+} cell populations and their percentages, respectively. (*F*) Quantitative RT-PCR analysis for expression of PCLP1 and Msln in freshly isolated E12.5 PCLP1^{high} cells and cultured MCs. The actual ratios of marker/GAPDH in PLCP1^{high} cells and cultured cells (+OSM bFGF or −OSM bFGF) are as follows: PCLP1, 2.1×10^{-1}, 8.0×10^{-2}, and 7.5×10^{-3}; Msln, 1.8×10^{-3}, 6.6×10^{-2}, and 3.0×10^{-1}. $^{*}P < .00003$; Student *t* test.

Fetal Hepatic MCs Are a Rich Source of Growth Factors for Hepatoblasts

It is known that MCs possess characteristics of both epithelial and mesenchymal cells,[7] but precise information about gene expression and other developmental characteristics of MCs remains limited. Therefore, microarray analysis was performed to compare gene expression profiles of E12.5 PCLP1^{high}Msln^{-} MC progenitors with adult Msln^{+} MCs (National Center for Biotechnology Information Gene Expression Omnibus accession no. GSE 18937). We found that MCs changed their gene expression profile drastically dur-

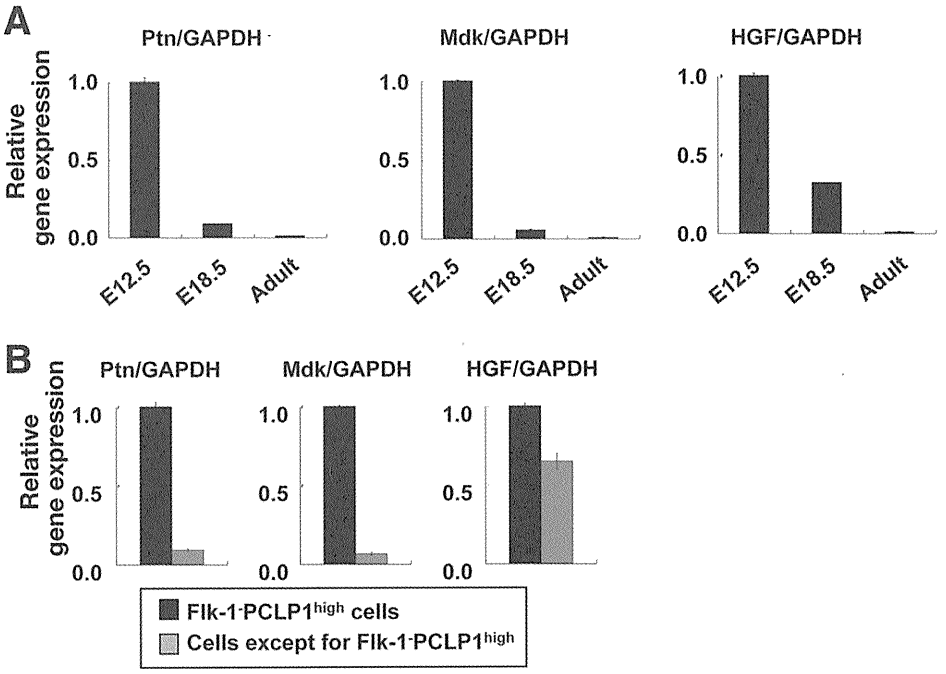

Figure 4. Expression of growth factors in liver cells. (*A*) Quantitative RT-PCR analysis for growth factors in MCs at distinct developmental stages. E12.5 Flk1^{-}PCLP1^{high} cells, E18.5 Msln^{+} cells, and adult Msln^{+} cells were isolated by a cell sorter and used for analyses. The actual ratios of factor/GAPDH in E12.5, E18.5, and adult MCs are as follows: Ptn, 3.9×10^{-1}, 4.0×10^{-2}, and 2.9×10^{-3}; Mdk, 1.0×10^{-1}, 6.1×10^{-3}, and 5.1×10^{-4}; HGF, 2.6×10^{-3}, 1.1×10^{-3}, and 4.7×10^{-4}. (*B*) Quantitative RT-PCR analysis of growth factors in Flk1^{-}PCLP1^{high} cells and the other cells at E12.5. The actual ratios of growth factor/GAPDH in Flk1^{-}PCLP1^{high} cells and the other cells are as follows: Ptn, 3.9×10^{-1} and 4.1×10^{-2}; Mdk, 1.0×10^{-1} and 7.8×10^{-3}; HGF, 2.6×10^{-3} and 1.6×10^{-3}.

ing development and that various signaling molecules were expressed in both fetal and adult MCs. In the list of soluble mediators whose expression in E12.5 MCs was more than 5-fold higher than in adult MCs (Supplementary Table 1), there were several growth factors known to promote proliferation of hepatocytes. Ptn is known to be a mitogen for adult hepatocytes[4,5] and was shown to be expressed highly in the STM and the hepatic MC layer of rat embryos.[5] Mdk is a molecule structurally related to Ptn.[4] Consistent with the microarray analysis, quantitative reverse-transcription (RT)-PCR analysis revealed that Ptn and Mdk were highly expressed in E12.5 MCs and became gradually down-regulated during ontogeny (Figure 4*A*). HGF was also expressed in E12.5 MCs, although its expression level was much lower than those of Ptn and Mdk (see the legend for Figure 4*A*). Furthermore, these growth factors were expressed more abundantly in MCs at E12.5 compared with non-MCs that contained hepatocytes, ECs, mesenchymal cells, and blood cells (Figure 4*B*). The expression of insulin-like growth factor 2 was detected at high levels in fetal MCs, although it was also expressed in fetal hepatocytes (data not shown). Importantly, all of these factors were remarkably down-regulated during development and were hardly detectable in adult MCs (Figure 4*A*). These observations suggested the intriguing possibility that fetal hepatic MCs play an active role in the proliferation and/or differentiation of hepatic cells in the developing liver.

Fetal MCs Promote Expansion of Hepatoblasts in a Paracrine Manner by Secreting Soluble Factors

To examine whether fetal MCs contribute to proliferation of hepatoblasts, we designed a coculture system of fetal hepatocytes with fetal MCs. Because the number of MCs isolated from fetal livers was too small for such experiments, we took advantage of fetal MCs expanded in vitro. Fetal hepatoblasts were isolated from E14.5 livers with anti-Dlk1 Ab as reported previously[18] and cultured with or without fetal MCs expanded in vitro using a 3-μm pored Transwell (Figure 5*A*). Hepatoblasts proliferated actively in the presence of Ptn or Mdk (Figure 5*B*) and in the coculture with MCs (Figure 5*C* and *D*), which was confirmed by WST-1 assay. MCs isolated from a later stage (E18.5) also enhanced the proliferation of fetal hepatocytes, and E16.5 hepatocytes also proliferated by coculture with later-stage MCs (Supplementary Figure 3 and data not shown). Importantly, MCs cultured without OSM and bFGF before coculture failed to stimulate the proliferation of hepatoblasts (Figure 5*C*). These MCs also exhibited a cell surface phenotype similar to differentiated MCs (Figure 3*E* and *F*), and growth factor expression was remarkably reduced, similar to adult MCs (Figures 5*E* and 4*A*). By contrast, MCs cultured in the presence of OSM and bFGF expressed growth factors at levels comparable to E18.5 MCs (Figures 5*E* and 4*A*). These results indicated that fetal hepatic MCs possess the potential to promote the proliferation of hepatocytes by secreting soluble factors, and the 2 types of MCs used for coculture exhibit the characteristics of fetal undifferentiated MCs and adult MCs in vivo, respectively.

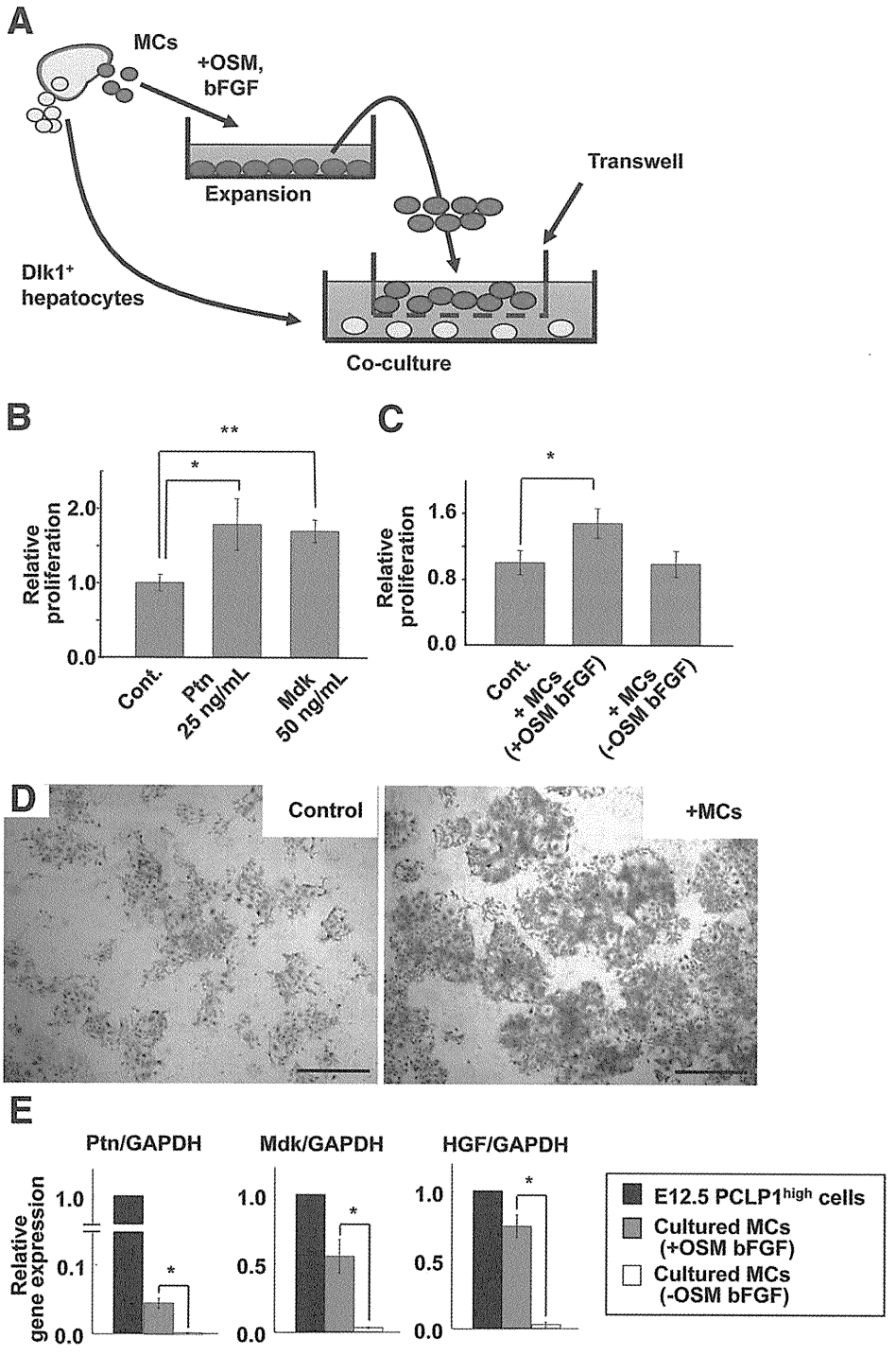

Figure 5. Hepatic MCs promote the proliferation of hepatoblasts in the coculture system. (*A*) The coculture system of fetal hepatoblasts and hepatic MCs separated by Transwell. After culturing of freshly isolated MCs in the presence of OSM and bFGF, the expanded MCs were used for coculture with Dlk1$^+$ hepatoblasts. (*B*) Proliferation of hepatoblasts in coculture system. Dlk1$^+$ cells sorted from E14.5 livers were cultured in the presence of growth factors as indicated. Growth of hepatocytes was measured by WST-1 assay after 4 days of culture. The averages for 3 wells of each sample are shown. $^*P < .03$; $^{**}P < .004$; Student *t* test. (*C*) Proliferation of E14.5 Dlk1$^+$ cells cultured with in vitro expanded E12.5 MCs. After primary expansion of MCs, the cells were cultured for an additional 5 days in the presence or absence of OSM and bFGF before coculture. Growth of hepatocytes was measured by WST-1 assay as in *B*. $^*P < .007$; Student *t* test. (*D*) Appearance of hepatocytes stained with Giemsa solution after 3 days of coculture. (*E*) Quantitative RT-PCR analysis of growth factors in freshly isolated E12.5 PCLP1^{high} cells and cultured MCs. The actual ratios of marker/GAPDH in PLCP1^{high} cells and cultured cells with OSM and bFGF (+OSM bFGF) or without them (−OSM bFGF) before coculture are as follows: Ptn, $1.4, 5.7 \times 10^{-2}$, and 2.6×10^{-3}; Mdk, 1.8×10^{-2}, 1.0×10^{-2}, and 5.5×10^{-4}; HGF, 4.1×10^{-4}, 3.0×10^{-4}, and 1.1×10^{-5}. $^*P < .0005$; Student *t* test.

In Vivo Function of Fetal Hepatic MCs

Wilms' tumor 1 homologue (WT1) is a Zn finger protein that is known to play a critical role in organogenesis of multiple organs, including the kidney, heart, diaphragm, spleen, gonad, and liver. WT1 is also known as a marker for the mesothelial lineage,[7] and it is believed to be a regulator of mesothelial development. In mouse fetal liver, WT1 was reported to be expressed strongly in coelomic epithelial cells,[21] which correspond to hepatic MCs. In fact, WT1 was mainly expressed in MCs, whereas its expression was hardly detectable in non-MCs, including hepatocytes, ECs, mesenchymal cells, and blood cells

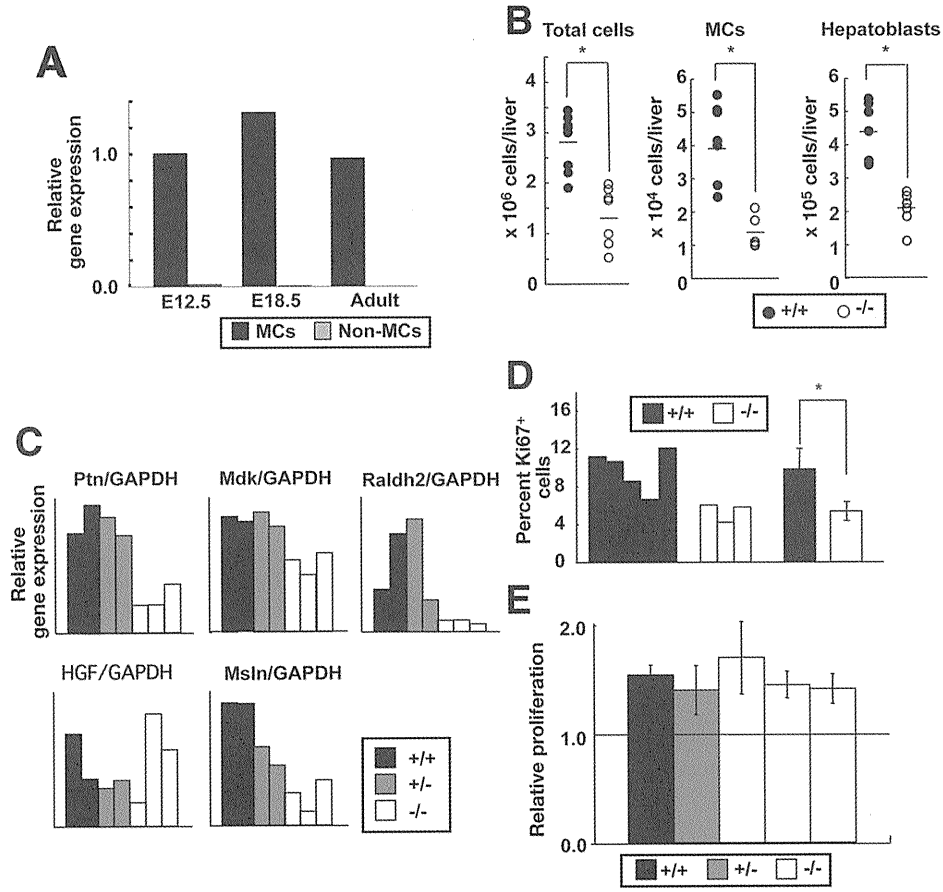

Figure 6. Characteristics of hepatic MCs in WT1-deficient embryos. (*A*) Quantitative RT-PCR analysis of WT1 expression in MCs or non-MCs. The relative gene expression of WT1/GAPDH in MCs and non-MCs at distinct developmental stages is shown. The actual ratios of WT1/GAPDH in MCs and non-MCs for E12.5, E18.5, and adults are 2.4×10^{-4} and 3.2×10^{-6}, 3.7×10^{-4} and 3.5×10^{-7}, and 2.3×10^{-4} and 2.8×10^{-6}, respectively. (*B*) The numbers of total fetal liver cells (*left panel*; +/+, n = 8; −/−, n = 8), PCLP1^{high} cells (*middle panel*; +/+, n = 7; −/−, n = 6), and Dlk1^{+} cells (right panel, +/+, n = 7; −/−, n = 6) per liver of E13.5 embryos are shown. *$P < .0007$; Student *t* test. (*C*) Quantitative RT-PCR analysis in PCLP1^{high} MCs of E13.5 littermates. Relative gene expression is shown. *Filled*, *gray*, and *open bars* indicate an individual embryo with +/+, +/−, and −/− genotype, respectively. (*D*) The ratio of Ki67^{+} cells in PCLP1^{high} MCs between E13.5 WT1$^{+/+}$ and WT1$^{-/-}$ livers of littermates. The *right bars* show the difference between the 2 genotypes. *$P < .02$; Student *t* test. (*E*) Proliferation potential of Dlk1^{+} hepatoblasts derived from E13.5 WT1$^{+/+}$, WT1$^{+/-}$, and WT1$^{-/-}$ livers. Dlk1^{+} hepatoblasts of littermates with each genotype were sorted by a cell sorter and cocultured with or without in vitro expanded E12.5 WT1$^{+/+}$ MCs. Growth of hepatocytes was measured by WST-1 assay in triplicate cultures after 4 days of coculture. The ratios of the WST-1 value in culture with MCs to that without MCs are shown for each genotype. Note that there is no significant difference among genotypes. The experiment was repeated twice with similar results.

in the developing liver (Figure 6*A*). Consistent with a previous report,[21] WT1$^{-/-}$ embryos had smaller livers with incomplete lobulation compared with littermates with WT1$^{+/+}$ or WT1$^{+/-}$ genotypes at E13.5 (Supplementary Figure 4*A* and data not shown). The percentages of Flk1^{-}PCLP1^{high} MC progenitors in WT1$^{-/-}$ fetal livers were not reduced significantly compared with their littermates by flow cytometry (Supplementary Figure 4*B* and data not shown). However, the numbers of Flk1^{-}PCLP1^{high} MCs, Dlk1^{+} hepatoblasts, and total fetal liver cells were all reduced in WT1$^{-/-}$ animals (Figure 6*B*). Next, we isolated MCs to examine the expression of growth factors by quantitative RT-PCR. Ptn and Mdk were reduced in WT1$^{-/-}$ hepatic MCs compared with the littermates with WT1$^{+/+}$ or WT1$^{+/-}$ genotypes (Figure 6*C*). The expression of Msln in WT1$^{-/-}$ MCs was also severely reduced at E13.5, indicating that MC differentiation may also be impaired in WT1-deficient livers. In addition, the expression of retinaldehyde dehydrogenase 2 (RALDH2) was significantly reduced in WT1$^{-/-}$ MCs, consistent with the notion that retinoic acid regulates proliferation of MCs in vivo.[21] Proliferation of MCs might also be altered in these embryos. The percentages of Ki67^{+} cells in PCLP1^{high} MCs isolated from WT1$^{-/-}$ embryos were significantly reduced compared with those of WT1$^{+/+}$ embryos (Figure 6*D*). Coculture of Dlk1^{+}

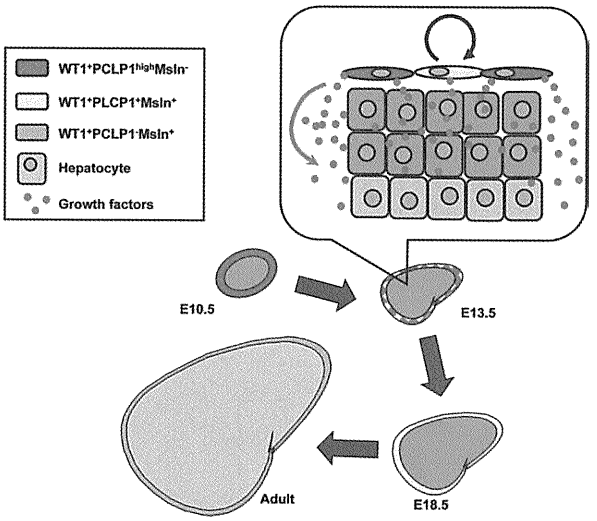

Figure 7. A model for hepatic MC development and its role in liver organogenesis. At an early stage of liver development, PCLP1^{high}Msln^{-} immature MCs cover the hepatic lobes (E10.5–12.5, *red*). The expression of Msln is up-regulated in MCs during fetal liver development, and most of the MCs become PCLP1^{+}Msln^{+} around birth (E18.5, *light yellow*). MCs provide hepatoblasts with multiple growth factors and they also proliferate actively during fetal stages, contributing to liver organogenesis. After birth, MCs become PCLP1^{-}Msln^{+} (*light green*), and their proliferation potential declines. MCs then switch their function from a niche for hepatoblasts to nonadhesive protective surfaces.

hepatocytes from WT1$^{-/-}$ or WT1$^{+/+}$ livers with WT1$^{+/+}$ MCs showed no significant difference in proliferation of hepatocytes among the different genotypes, indicating that the reduced proliferation of hepatocytes in WT1$^{-/-}$ fetal livers was not due to defects in hepatocytes (Figure 6*E*). From these results, we concluded that WT1-null hepatic MCs are defective in proliferation and the production of growth factors. These results strongly suggested that impaired development of hepatic MCs results in decreased proliferation of hepatocytes as well as abnormal morphogenesis of the liver.

Discussion

In this study, we show that splanchnic MCs are not only an inert protective sheet for coelomic organs but also change their characteristics dynamically during organogenesis. In the liver, at least 3 distinct developmental stages of MCs are recognized based on the expression of PCLP1 and Msln (Figure 7). PCLP1^{high}Msln^{-} immature MC progenitors at E10.5 define the border of each hepatic lobe. Furthermore, the proliferation and gene expression profile of hepatic MCs change dramatically during development. In particular, fetal hepatic MCs were shown to express various soluble factors, including hepatocyte mitogens such as Ptn, Mdk, and HGF, indicating that MCs function as a rich source of growth factors for hepatic cells in liver development (Figures 4 and 7). In fact, coculture experiments using MCs and Dlk1^{+} fetal hepatocytes clearly show that MCs provide growth factors for hepatocytes. Considering that mesenchymal cells derived from STM contribute to the commitment of foregut endodermal cells into the hepatic lineage and to the outgrowth of hepatoblasts at the onset of liver development, it is not surprising that the lateral plate mesoderm-derived mesothelial tissue plays an active role in liver development as a producer of growth factors. Consistent with the previous report by Suksaweang et al,[6] we observed that Ki67^{+}HNF4α^{+} proliferating hepatocytes were present more frequently in the peripheral region than in the central region of the lobes in developing mouse liver (Supplementary Figure 5 and Supplementary Table 2). These observations suggest that MCs contribute to liver growth and morphogenesis by providing mitotic stimuli and/or microenvironment for hepatocytes.

This idea is strongly supported by the analysis of WT1-deficient mice. Ijpenberg et al recently reported that the livers of WT1 mutant embryos are small, showing defects in the proliferation of coelomic epithelial cells and hepatocytes, lobulation, and differentiation of stellate cells during liver development.[21] Coelomic epithelial cells lining the liver of WT1-null embryos showed the reduction of Raldh2 expression, suggesting possible involvement of the retinoic acid signaling pathway in liver development as in the case of heart development that requires WT1-expressing epicardial cells and Raldh2.[22,23] However, it had been unclear why proliferation of hepatocytes was also impaired in WT1-deficient fetal livers. Isolation and characterization of PCLP1^{high} MCs from WT1$^{-/-}$ mice in this study show that proliferation of MCs and their production of growth factors, including Ptn and Mdk, are impaired in these embryos, whereas Dlk1^{+} cells from WT1$^{-/-}$ livers proliferate normally in response to WT1$^{+/+}$ MCs. The expression level of HGF was not affected in the absence of WT1, although the expression level of HGF in WT1$^{+/+}$ MCs was much lower than that of Ptn and Mdk. Thus, it is strongly suggested that the growth retardation of WT1-deficient livers is mainly due to the reduced proliferation of hepatic MCs and their insufficient production of mitogens for hepatocytes. Importantly, because MCs express various growth factors, there might be factors other than Ptn, Mdk, and HGF that also stimulate proliferation of hepatocytes.

Previous studies showed that WT1-expressing epicardial and serosal MCs are a source of coronary and gut vasculogenic cells, respectively.[8,10] It is thus of great interest to know whether immature PCLP1^{high}Msln^{-} cells also possess the potential to differentiate into nonmesothelial lineages. In fact, Pérez-Pomares et al reported that liver sinusoidal endothelial cells and mural cells in avian embryos were derived from the mesothelium.[11] We observed that some ALCAM^{+} cells were generated in the culture of E12.5 PCLP1^{high}ALCAM^{-} MCs (Supplemen-

tary Figure 6). Because ALCAM is specifically expressed in submesothelial cells that underlie the hepatic MC layer,[24] MCs may have a potential to give rise to those mesenchymal cells. Further studies on the differentiation potential of MCs may provide new insights in liver organogenesis.

Fetal liver is the major hematopoietic organ and contains numerous blood cells, which also contribute to hepatogenesis. We previously showed that OSM produced from blood cells stimulates the differentiation of fetal hepatoblasts in vitro.[25] After birth, hematopoiesis shifts to the bone marrow and OSM expression decreases in the liver. In this report, we show that OSM stimulates the proliferation of fetal hepatic MCs and maintains their immature characteristics, including the ability to support the proliferation of hepatoblasts. These results suggest the possible link between hematopoiesis and the proliferation of MCs and hepatoblasts in fetal liver and that OSM may play a role for the coordination of these cells.

In conclusion, this study reveals dynamic changes in characteristics of hepatic MCs during development and shows that hepatic MCs play an active role in organogenesis by providing growth factors for parenchymal cells. Besides liver development, fetal MCs may also be actively involved in the development of other organs.

Supplementary Material

Note: To access the supplementary material accompanying this article, visit the online version of *Gastroenterology* at www.gastrojournal.org, and at doi: 10.1053/j.gastro.2009.12.059.

References

1. Jung J, Zheng M, Goldfarb M, et al. Initiation of mammalian liver development from endoderm by fibroblast growth factors. Science 1999;284:1998–2003.
2. Rossi JM, Dunn NR, Hogan BL, et al. Distinct mesodermal signals, including BMPs from the septum transversum mesenchyme, are required in combination for hepatogenesis from the endoderm. Genes Dev 2001;15:1998–2009.
3. Matsumoto K, Yoshitomi H, Rossant J, et al. Liver organogenesis promoted by endothelial cells prior to vascular function. Science 2001;294:559–563.
4. Muramatsu T. Midkine and pleiotrophin: two related proteins involved in development, survival, inflammation and tumorigenesis. J Biochem 2002;132:359–371.
5. Asahina K, Sato H, Yamasaki C, et al. Pleiotrophin/heparin-binding growth-associated molecule as a mitogen of rat hepatocytes and its role in regeneration and development of liver. Am J Pathol 2002;160:2191–2205.
6. Suksaweang S, Lin CM, Jiang TX, et al. Morphogenesis of chicken liver: identification of localized growth zones and the role of beta-catenin/Wnt in size regulation. Dev Biol 2004;266:109–122.
7. Herrick SE, Mutsaers SE. Mesothelial progenitor cells and their potential in tissue engineering. Int J Biochem Cell Biol 2004;36:621–642.
8. Perez-Pomares JM, Carmona R, Gonzalez-Iriarte M, et al. Origin of coronary endothelial cells from epicardial mesothelium in avian embryos. Int J Dev Biol 2002;46:1005–1013.
9. Que J, Wilm B, Hasegawa H, et al. Mesothelium contributes to vascular smooth muscle and mesenchyme during lung development. Proc Natl Acad Sci U S A 2008;105:16626–16630.
10. Wilm B, Ipenberg A, Hastie ND, et al. The serosal mesothelium is a major source of smooth muscle cells of the gut vasculature. Development 2005;132:5317–5328.
11. Pérez-Pomares JM, Carmona R, Gonzalez-Iriarte M, et al. Contribution of mesothelium-derived cells to liver sinusoids in avian embryos. Dev Dyn 2004;229:465–474.
12. Kerjaschki D, Sharkey DJ, Farquhar MG. Identification and characterization of podocalyxin—the major sialoprotein of the renal glomerular epithelial cell. J Cell Biol 1984;98:1591–1596.
13. Horvat R, Hovorka A, Dekan G, et al. Endothelial cell membranes contain podocalyxin—the major sialoprotein of visceral glomerular epithelial cells. J Cell Biol 1986;102:484–491.
14. Hara T, Nakano Y, Tanaka M, et al. Identification of podocalyxin-like protein 1 as a novel cell surface marker for hemangioblasts in the murine aorta-gonad-mesonephros region. Immunity 1999;11:567–578.
15. Doyonnas R, Nielsen JS, Chelliah S, et al. Podocalyxin is a CD34-related marker of murine hematopoietic stem cells and embryonic erythroid cells. Blood 2005;105:4170–4178.
16. Rump A, Morikawa Y, Tanaka M, et al. Binding of ovarian cancer antigen CA125/MUC16 to mesothelin mediates cell adhesion. J Biol Chem 2004;279:9190–9198.
17. Kreidberg JA, Sariola H, Loring JM, et al. WT-1 is required for early kidney development. Cell 1993;74:679–691.
18. Tanimizu N, Nishikawa M, Saito H, et al. Isolation of hepatoblasts based on the expression of Dlk/Pref-1. J Cell Sci 2003;116:1775–1786.
19. Tanaka M, Okabe M, Suzuki K, et al. Mouse hepatoblasts at distinct developmental stages are characterized by expression of EpCAM and DLK1: drastic change of EpCAM expression during liver development. Mech Dev 2009;126:665–676.
20. Suzuki K, Tanaka M, Watanabe N, et al. p75 Neurotrophin receptor is a marker for precursors of stellate cells and portal fibroblasts in mouse fetal liver. Gastroenterology 2008;135:270–281, e3.
21. Ijpenberg A, Perez-Pomares JM, Guadix JA, et al. Wt1 and retinoic acid signaling are essential for stellate cell development and liver morphogenesis. Dev Biol 2007;312:157–170.
22. Niederreither K, Subbarayan V, Dolle P, et al. Embryonic retinoic acid synthesis is essential for early mouse post-implantation development. Nat Genet 1999;21:444–448.
23. Perez-Pomares JM, Phelps A, Sedmerova M, et al. Experimental studies on the spatiotemporal expression of WT1 and RALDH2 in the embryonic avian heart: a model for the regulation of myocardial and valvuloseptal development by epicardially derived cells (EPDCs). Dev Biol 2002;247:307–326.
24. Asahina K, Tsai SY, Li P, et al. Mesenchymal origin of hepatic stellate cells, submesothelial cells, and perivascular mesenchymal cells during mouse liver development. Hepatology 2009;49:998–1011.
25. Kinoshita T, Sekiguchi T, Xu MJ, et al. Hepatic differentiation induced by oncostatin M attenuates fetal liver hematopoiesis. Proc Natl Acad Sci U S A 1999;96:7265–7270.

Received June 30, 2009. Accepted December 31, 2009.

Reprint requests

Address requests for reprints to: Atsushi Miyajima, PhD, Laboratory of Cell Growth and Differentiation, Institute of Molecular